CHAPTER

9

FIBER OPTICS

Charles Kao (born 1933) promulgated the concept of using low-loss optical fibers in practical telecommunications systems.

Philip St John Russell (born 1953) invented the photonic-crystal fiber in 1991; it has found use in many applications.

An optical fiber is a cylindrical dielectric waveguide made of a low-loss material, such as silica glass. It has a central **core** in which the light is guided, embedded in an outer **cladding** of slightly lower refractive index (Fig. 9.0-1). Light rays incident on the core–cladding boundary at angles greater than the critical angle undergo total internal reflection and are guided through the core without refraction into the cladding. Rays at greater inclination to the fiber axis lose part of their power into the cladding at each reflection and are not guided.

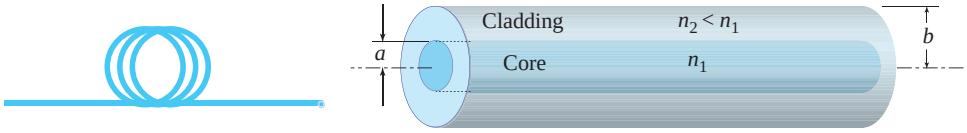

Figure 9.0-1 An optical fiber is a cylindrical dielectric waveguide with an inner core and an outer cladding.

Remarkable technological advances in the fabrication of optical fibers over the past two decades allow light to be guided through 1 km of glass fiber with a loss as low as ≈ 0.15 dB ($\approx 3.4\%$) at the wavelength of maximum transparency. Because of this low loss, optical fibers long ago replaced copper coaxial cables as the preferred transmission medium for terrestrial and sub-oceanic voice and data communications.

In this chapter we introduce the principles of light transmission in optical fibers. These principles are essentially the same as those applicable to planar dielectric waveguides (Chapter 8); the most notable distinction is that optical fibers have cylindrical geometry. In both types of waveguide, light propagates in the form of modes. Each mode travels along the axis of the waveguide with a distinct propagation constant and group velocity, maintaining its transverse spatial distribution and polarization. In a planar dielectric waveguide, each mode is described as the sum of the multiple reflections of a TEM wave bouncing within the slab, in the direction of an optical ray at a certain bounce angle. This approach is approximately applicable to cylindrical waveguides as well. When the core diameter is small, only a single mode is supported and the fiber is said to be a **single-mode fiber**.

Fibers with large core diameters are **multimode fibers**. One of the difficulties associated with the propagation of light in a multimode fiber arises from the differences among the group velocities of the modes. This results in a spread of travel times and results in the broadening of a light pulse as it travels through the fiber. This effect, called **modal dispersion**, limits how often adjacent pulses can be launched without resulting in pulse overlap at the far end of the fiber. Modal dispersion therefore limits the speed at which multimode optical fiber communications systems can operate.

Modal dispersion can be reduced by grading the refractive index of the fiber core from a maximum value at its center to a minimum value at the core–cladding boundary. The fiber is then called a **graded-index fiber**, or **GRIN** fiber, whereas conventional fibers with constant refractive indexes in the core and the cladding are known as **step-index fibers**. In a graded-index fiber the travel velocity increases with radial distance from the core axis (since the refractive index decreases). Although rays of greater inclination to the fiber axis must travel farther, they thus travel faster. This permits the travel times of the different modes to be equalized.

In summary, optical fibers are classified as step-index or graded-index, and multimode or single-mode, as illustrated in Fig. 9.0-2.

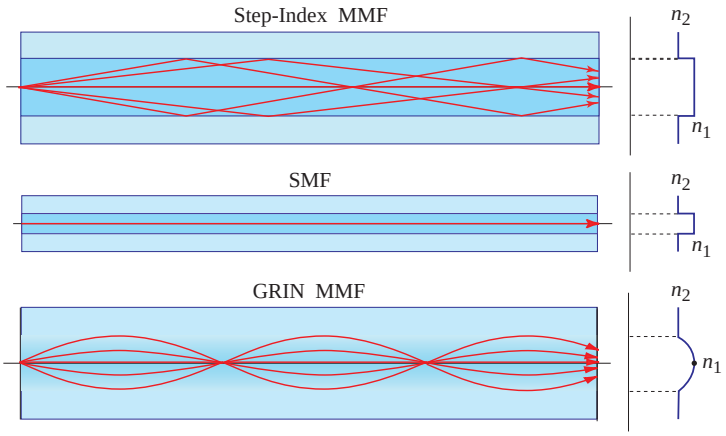

Figure 9.0-2 Geometry, refractive-index profile, and typical rays in a step-index multimode fiber (MMF), a single-mode fiber (SMF), and a graded-index multimode fiber (GRIN MMF).

This Chapter

This chapter begins with ray-optics descriptions of step-index and graded-index fibers (Sec. 9.1). An electromagnetic-optics approach, emphasizing the nature of optical modes and single-mode propagation, follows in Sec. 9.2. The optical properties of the fiber material (usually fused silica), including attenuation and material dispersion, as well as modal, waveguide, and polarization-mode dispersion, are discussed in Sec. 9.3. Since fibers are usually used to transmit information in the form of optical pulses, a brief introduction to pulse propagation in fibers is also provided in Sec. 9.3. Holey and photonic-crystal fibers, which have more complex refractive-index profiles, and unusual dispersion characteristics, are introduced in Sec. 9.4. We return to this topic in Chapters 22 and 24, which are devoted to ultrafast optics and optical fiber communications systems, respectively.

9.1 GUIDED RAYS

A. Step-Index Fibers

A step-index fiber is a cylindrical dielectric waveguide specified by the refractive indexes of its core and cladding, n_1 and n_2, respectively, and their radii a and b (see Fig. 9.0-1). Examples of standard core-to-cladding diameter ratios (in units of $\mu\text{m}/\mu\text{m}$) are $2a/2b = 8/125, 50/125, 62.5/125, 85/125$, and $100/140$. The refractive indexes of the core and cladding differ only slightly, so that the fractional refractive-index change is small:

$$\Delta \equiv \frac{n_1^2 - n_2^2}{2n_1^2} \approx \frac{n_1 - n_2}{n_1} \ll 1. \tag{9.1-1}$$

Most fibers used in currently implemented optical communication systems are made of fused silica glass (SiO_2) of high chemical purity. Slight changes in the refractive index are effected by adding low concentrations of doping materials (e.g., titanium, germanium, boron). The refractive index n_1 ranges from 1.44 to 1.46, depending on the wavelength, and Δ typically lies between 0.001 and 0.02.

An optical ray in a step-index fiber is guided by total internal reflections within the fiber core if its angle of incidence at the core–cladding boundary is greater than the critical angle $\theta_c = \sin^{-1}(n_2/n_1)$, and remains so as the ray bounces.

Meridional Rays

Meridional rays, which are rays confined to planes that pass through the fiber axis, have a particularly simple guiding condition, as shown in Fig. 9.1-1. These rays intersect the fiber axis and reflect in the same plane without changing their angle of incidence, behaving as if they were in a planar waveguide. Meridional rays are guided if the angle θ they make with the fiber axis is smaller than the complement of the critical angle, i.e., if $\theta < \overline{\theta}_c = \pi/2 - \theta_c = \cos^{-1}(n_2/n_1)$. Since $n_1 \approx n_2$, $\overline{\theta}_c$ is usually small and the guided rays are approximately paraxial.

Figure 9.1-1 The trajectory of a meridional ray lies in a plane that passes through the fiber axis. The ray is guided if $\theta < \overline{\theta}_c = \cos^{-1}(n_2/n_1)$.

Skewed Rays

An arbitrary ray is identified by its plane of incidence, which is a plane parallel to the fiber axis through which the ray passes, and by the angle with that axis, as illustrated in Fig. 9.1-2. The plane of incidence intersects the core–cladding cylindrical boundary at an angle ϕ with respect to the normal to the boundary and lies at a distance R from the fiber axis. The ray is identified by its angle θ with the fiber axis and by the angle ϕ of its plane. When $\phi \neq 0$ ($R \neq 0$) the ray is said to be skewed. For meridional rays $\phi = 0$ and $R = 0$.

A skewed ray reflects repeatedly into planes that make the same angle ϕ with the core–cladding boundary; it follows a helical trajectory confined within a cylindrical shell of inner and outer radii R and a, respectively, as illustrated in Fig. 9.1-2. The projection of the trajectory onto the transverse (x–y) plane is a regular polygon that is not necessarily closed. The condition for a skewed ray to always undergo total internal reflection is that its angle with the z axis be smaller than the complementary critical angle, i.e., $\theta < \overline{\theta}_c$.

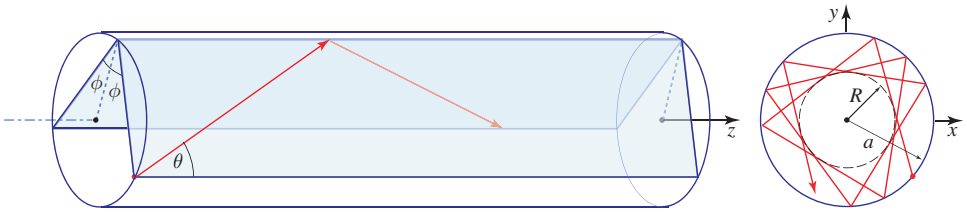

Figure 9.1-2 A skewed ray lies in a plane offset from the fiber axis by a distance R. The ray is identified by the angles θ and ϕ. It follows a helical trajectory confined within a cylindrical shell with inner and outer radii R and a, respectively. The projection of the ray on the transverse plane is a regular polygon that is not necessarily closed.

Numerical Aperture

A ray incident from air into the fiber becomes a guided ray if, upon refraction into the core, it makes an angle θ with the fiber axis that is smaller than $\overline{\theta}_c$. As shown in Fig. 9.1-3(a), if Snell's law is applied at the air–core boundary, the angle θ_a in air corresponding to the angle $\overline{\theta}_c$ in the core is obtained from $1 \cdot \sin\theta_a = n_1 \sin\overline{\theta}_c$, which leads to $\sin\theta_a = n_1\sqrt{1-\cos^2\overline{\theta}_c} = n_1\sqrt{1-(n_2/n_1)^2} = \sqrt{n_1^2 - n_2^2}$ (see Exercise 1.2-5). The acceptance angle of the fiber is therefore

$$\theta_a = \sin^{-1} \mathrm{NA}, \tag{9.1-2}$$

where the numerical aperture (NA) of the fiber is given by

$$\boxed{\mathrm{NA} = \sqrt{n_1^2 - n_2^2} \approx n_1\sqrt{2\Delta}} \qquad \begin{matrix}(9.1\text{-}3)\\ \text{Numerical Aperture}\end{matrix}$$

since $n_1 - n_2 = n_1\Delta$ and $n_1 + n_2 \approx 2n_1$.

The acceptance angle θ_a of the fiber determines the cone of external rays that are guided by the fiber. Rays incident at angles greater than θ_a are refracted into the fiber but are guided only for a short distance since they do not undergo total internal reflection. The numerical aperture therefore describes the light-gathering capacity of the fiber, as illustrated in Fig. 9.1-3(b).

When the guided rays arrive at the terminus of the fiber, they are refracted back into a cone of angle θ_a. The acceptance angle is thus a crucial design parameter for coupling light into and out of a fiber.

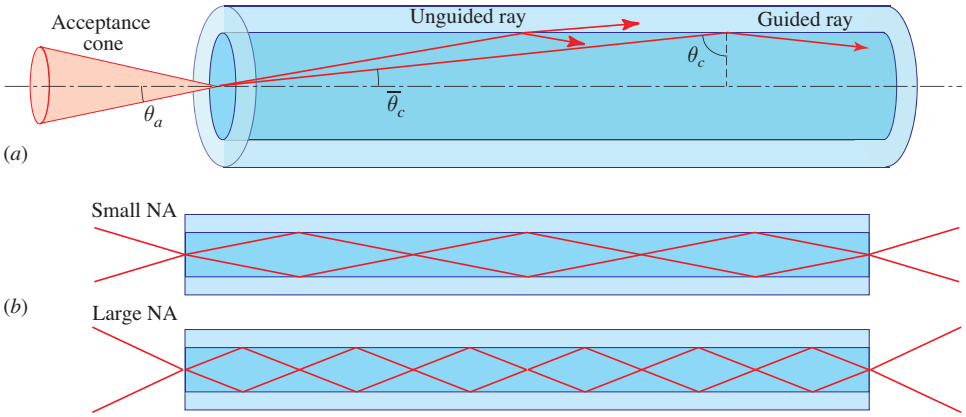

Figure 9.1-3 (a) The acceptance angle θ_a of a fiber. Rays within the acceptance cone are guided by total internal reflection. The numerical aperture $\mathrm{NA} = \sin\theta_a$. The angles θ_a and $\overline{\theta}_c$ are typically quite small; they are exaggerated here for clarity. (b) The light-gathering capacity of a large NA fiber is greater than that of a small NA fiber.

EXAMPLE 9.1-1. ***Cladded and Uncladded Fibers.*** In a silica-glass fiber with $n_1 = 1.46$ and $\Delta = (n_1 - n_2)/n_1 = 0.01$, the complementary critical angle $\overline{\theta}_c = \cos^{-1}(n_2/n_1) = 8.1°$, and the acceptance angle $\theta_a = 11.9°$, corresponding to a numerical aperture $\mathrm{NA} = 0.206$. By

comparison, a fiber with silica-glass core ($n_1 = 1.46$) and a cladding with a much smaller refractive index $n_2 = 1.064$ has $\overline{\theta}_c = 43.2°$, $\theta_a = 90°$, and NA $= 1$. Rays incident from *all* directions are guided since they reflect within a cone of angle $\overline{\theta}_c = 43.2°$ inside the core. Likewise, for an uncladded fiber ($n_2 = 1$), $\overline{\theta}_c = 46.8°$, and rays incident from air at any angle are also refracted into guided rays. Although its light-gathering capacity is high, the uncladded fiber is generally not suitable for use as an optical waveguide because of the large number of modes it supports, as will be explained subsequently.

B. Graded-Index Fibers

Index grading is an ingenious method for reducing the pulse spreading caused by differences in the group velocities of the modes in a multimode fiber. The core of a graded-index (GRIN) fiber has a refractive index that varies; it is highest in the center of the fiber and decreases gradually to its lowest value where the core meets the cladding. The phase velocity of light is therefore minimum at the center and increases gradually with radial distance. Rays of the most axial mode thus travel the shortest distance, but they do so at the smallest phase velocity. Rays of the most oblique mode zigzag at a greater angle and travel a longer distance, but mostly in a medium where the phase velocity is high. The disparities in distances are thus compensated by opposite disparities in the phase velocities. As a consequence, the differences in the travel times associated with a light pulse are reduced. In this section we examine the propagation of light in GRIN fibers.

The core refractive index of a GRIN fiber is a function $n(r)$ of the radial position r. As illustrated in Fig. 9.1-4, the largest value of $n(r)$ is at the core center, $n(0) = n_1$, while the smallest value occurs at the core radius, $n(a) = n_2$. The cladding refractive index is maintained constant at n_2.

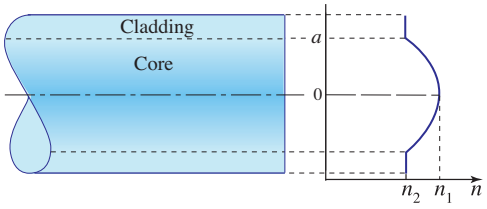

Figure 9.1-4 Geometry and refractive-index profile of a graded-index optical fiber.

A versatile refractive-index profile that exhibits this generic behavior is described as the power-law function

$$n^2(r) = n_1^2 \left[1 - 2\left(\frac{r}{a}\right)^p \Delta\right], \qquad r \le a, \tag{9.1-4}$$

where

$$\Delta = \frac{n_1^2 - n_2^2}{2n_1^2} \approx \frac{n_1 - n_2}{n_1}. \tag{9.1-5}$$

The **grade profile parameter** p determines the steepness of the profile. As illustrated in Fig. 9.1-5, $n^2(r)$ is a linear function of r for $p = 1$ and a quadratic function for $p = 2$. The quantity $n^2(r)$ becomes increasingly steep as p becomes larger, and ultimately approaches a step function for $p \to \infty$. The step-index fiber is thus a special case of the GRIN fiber.

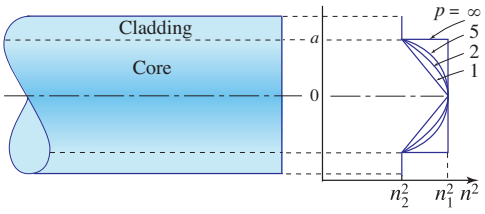

Figure 9.1-5 Power-law refractive-index profile $n_2(r)$ for various values of p.

The transmission of light rays through a GRIN medium with parabolic-index profile was discussed in Sec. 1.3. Rays in meridional planes follow oscillatory planar trajectories, whereas skewed rays follow helical trajectories with the turning points forming cylindrical caustic surfaces, as illustrated in Fig. 9.1-6. Guided rays are confined within the core and do not reach the cladding.

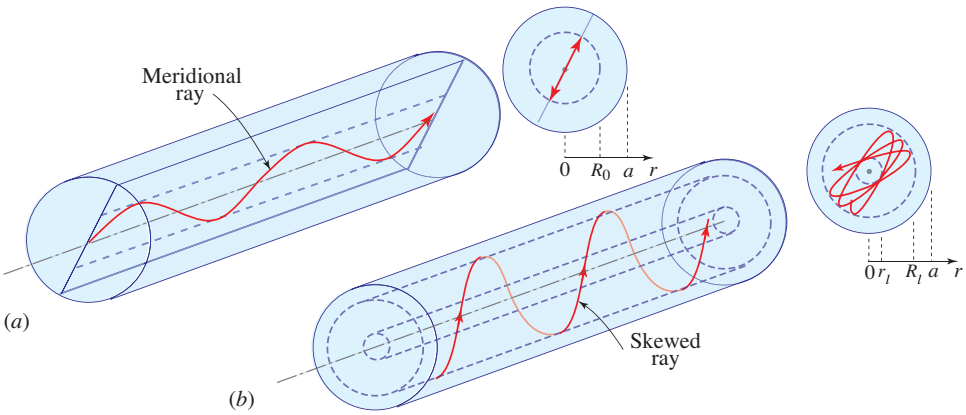

Figure 9.1-6 Guided rays in the core of a GRIN fiber. (a) A meridional ray confined to a meridional plane inside a cylinder of radius R_0. (b) A skewed ray follows a helical trajectory confined within two cylindrical shells of radii r_l and R_l.

The numerical aperture of a GRIN optical fiber may be determined by identifying the largest angle of the incident ray that is guided within the GRIN core without reaching the cladding. For meridional rays in a GRIN fiber with parabolic profile, the numerical aperture is given by (9.1-3) (see Exercise 1.3-2).

9.2 GUIDED WAVES

We now proceed to develop an electromagnetic-optics theory of light propagation in fibers. We seek to determine the electric and magnetic fields of guided waves by using Maxwell's equations and the boundary conditions imposed by the cylindrical dielectric core and cladding. As in all waveguides, there are certain special solutions, called modes (see Appendix C), each of which has a distinct propagation constant, a characteristic field distribution in the transverse plane, and two independent polarization states. Since an exact solution is rather difficult, a number of approximations will be used.

Helmholtz Equation

The optical fiber is a dielectric medium with refractive index $n(r)$. In a step-index fiber, $n(r) = n_1$ in the core $(r < a)$ and $n(r) = n_2$ in the cladding $(r > a)$. In a GRIN fiber, $n(r)$ is a continuous function in the core and has a constant value $n(r) = n_2$ in the cladding. In either case, we assume that the outer radius b of the cladding is sufficiently large so that it can be taken to be infinite when considering guided light in the core and near the core–cladding boundary.

Each of the components of the monochromatic electric and magnetic fields obeys the Helmholtz equation, $\nabla^2 U + n^2(r)k_o^2 U = 0$, where $k_o = 2\pi/\lambda_o$. This equation is obeyed exactly in each of the two regions of the step-index fiber, and is obeyed approximately within the core of the GRIN fiber if $n(r)$ varies slowly within a wavelength (see Sec. 5.3). In a cylindrical coordinate system (see Fig. 9.2-1) the Helmholtz equation is written as

$$\frac{\partial^2 U}{\partial r^2} + \frac{1}{r}\frac{\partial U}{\partial r} + \frac{1}{r^2}\frac{\partial^2 U}{\partial \phi^2} + \frac{\partial^2 U}{\partial z^2} + n^2 k_o^2 U = 0, \tag{9.2-1}$$

where $U = U(r, \phi, z)$. The guided modes are waves traveling in the z direction with propagation constant β, so that the z dependence of U is of the form $e^{-j\beta z}$. They are periodic in the angle ϕ with period 2π, so that they take the harmonic form $e^{-jl\phi}$, where l is an integer. Substituting

$$U(r, \phi, z) = u(r)e^{-jl\phi}e^{-j\beta z}, \qquad l = 0, \pm 1, \pm 2, \ldots \tag{9.2-2}$$

into (9.2-1) leads to an ordinary differential equation for the radial profile $u(r)$:

$$\frac{d^2 u}{dr^2} + \frac{1}{r}\frac{du}{dr} + \left(n^2(r)k_o^2 - \beta^2 - \frac{l^2}{r^2}\right)u = 0. \tag{9.2-3}$$

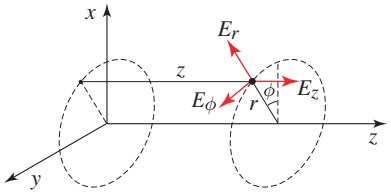

Figure 9.2-1 Cylindrical coordinate system.

A. Step-Index Fibers

As we found in Sec. 8.2B, the wave is guided (or bound) if the propagation constant is smaller than the wavenumber in the core $(\beta < n_1 k_o)$ and greater than the wavenumber in the cladding $(\beta > n_2 k_o)$. It is therefore convenient to define

$$k_T^2 = n_1^2 k_o^2 - \beta^2 \tag{9.2-4a}$$

and

$$\gamma^2 = \beta^2 - n_2^2 k_o^2, \tag{9.2-4b}$$

so that for guided waves k_T^2 and γ^2 are positive and k_T and γ are real. Equation (9.2-3) may then be written in the core and cladding separately:

$$\frac{d^2u}{dr^2} + \frac{1}{r}\frac{du}{dr} + \left(k_T^2 - \frac{l^2}{r^2}\right)u = 0, \qquad r < a \quad \text{(core)}, \tag{9.2-5a}$$

$$\frac{d^2u}{dr^2} + \frac{1}{r}\frac{du}{dr} - \left(\gamma^2 + \frac{l^2}{r^2}\right)u = 0, \qquad r > a \quad \text{(cladding)}. \tag{9.2-5b}$$

Equations (9.2-5) are well-known differential equations whose solutions are the family of Bessel functions. Excluding functions that approach ∞ at $r = 0$ in the core, or $r \to \infty$ in the cladding, we obtain the bounded solutions:

$$u(r) \propto \begin{cases} J_l(k_T r), & r < a \quad \text{(core)} \\ K_l(\gamma r), & r > a \quad \text{(cladding)}, \end{cases} \tag{9.2-6}$$

where $J_l(x)$ is the Bessel function of the first kind and order l, and $K_l(x)$ is the modified Bessel function of the second kind and order l. The function $J_l(x)$ oscillates like the sine or cosine function but with a decaying amplitude. The function $K_l(x)$ decays exponentially at large x. Two examples of the radial distribution $u(r)$ are displayed in Fig. 9.2-2.

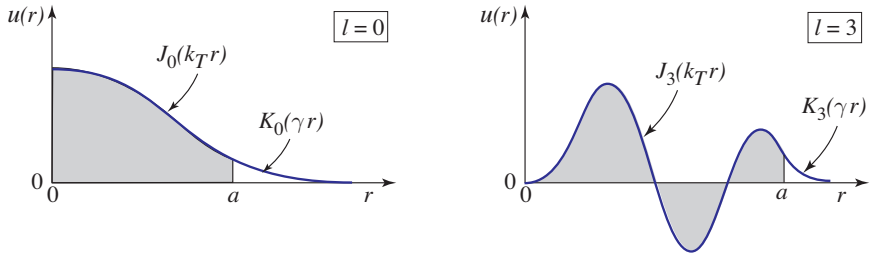

Figure 9.2-2 Examples of the radial distribution $u(r)$ provided in (9.2-6) for $l = 0$ and $l = 3$. The shaded and unshaded areas represent the fiber core and cladding, respectively. The parameters k_T and γ, and the two proportionality constants in (9.2-6), have been selected such that $u(r)$ is continuous and has a continuous derivative at $r = a$. Larger values of k_T and γ lead to a greater number of oscillations in $u(r)$.

The parameters k_T and γ determine the rate of change of $u(r)$ in the core and in the cladding, respectively. A large value of k_T means more oscillation of the radial distribution in the core. A large value of γ means more rapid decay and smaller penetration of the wave into the cladding. As can be seen from (9.2-4), the sum of the squares of k_T and γ is a constant,

$$k_T^2 + \gamma^2 = \left(n_1^2 - n_2^2\right)k_o^2 = (\text{NA})^2 \cdot k_o^2, \tag{9.2-7}$$

so that as k_T increases, γ decreases and the field penetrates deeper into the cladding. For those values of k_T that exceed $\text{NA} \cdot k_o$, the quantity γ becomes imaginary and the wave ceases to be bound to the core.

Fiber V Parameter

It is convenient to normalize k_T and γ by defining the quantities

$$X = k_T a, \qquad Y = \gamma a. \tag{9.2-8}$$

In view of (9.2-7),

$$X^2 + Y^2 = V^2, \tag{9.2-9}$$

where $V = \mathrm{NA} \cdot k_o a$, from which

$$\boxed{V = 2\pi \frac{a}{\lambda_o} \mathrm{NA}.} \tag{9.2-10}$$

V Parameter

It is important to keep in mind that for the wave to be guided, X must be smaller than V.

As we shall see shortly, V is an important parameter that governs the number of modes of the fiber and their propagation constants. It is called the **fiber parameter** or the V **parameter**. It is directly proportional to the radius-to-wavelength ratio a/λ_o, and to the numerical aperture NA. Equation (9.2-10) is not unlike (8.2-7) for the number of TE modes in a planar dielectric waveguide.

Modes

We now consider the boundary conditions. We begin by writing the axial components of the electric- and magnetic-field complex amplitudes, E_z and H_z, in the form of (9.2-2). The condition that these components must be continuous at the core–cladding boundary $r = a$ establishes a relation between the coefficients of proportionality in (9.2-6), so that we have only one unknown for E_z and one unknown for H_z. With the help of Maxwell's equations, $j\omega\epsilon_o n^2 \mathbf{E} = \nabla \times \mathbf{H}$ and $-j\omega\mu_o \mathbf{H} = \nabla \times \mathbf{E}$ [see (5.3-12) and (5.3-13)], the remaining four components, E_ϕ, H_ϕ, E_r, and H_r, are determined in terms of E_z and H_z. Continuity of E_ϕ and H_ϕ at $r = a$ yields two additional equations. One equation relates the two unknown coefficients of proportionality in E_z and H_z; the other provides a condition that the propagation constant β must satisfy. This condition, called the **characteristic equation** or **dispersion relation**, is an equation for β with the ratio a/λ_o and the fiber indexes n_1, n_2 as known parameters.

For each azimuthal index l, the characteristic equation has multiple solutions yielding discrete propagation constants β_{lm}, $m = 1, 2, \ldots$, each solution representing a mode. The corresponding values of k_T and γ, which govern the spatial distributions in the core and in the cladding, respectively, are determined by using (9.2-4) and are denoted k_{Tlm} and γ_{lm}. A mode is therefore described by the indexes l and m, characterizing its azimuthal and radial distributions, respectively. The function $u(r)$ depends on both l and m; $l = 0$ corresponds to meridional rays. Moreover, there are two independent configurations of the $\mathbf{E}$ and $\mathbf{H}$ vectors for each mode, corresponding to the two states of polarization. The classification and labeling of these configurations are generally quite involved (details are provided in specialized books in the reading list).

Characteristic Equation (Weakly Guiding Fiber)

Most fibers are weakly guiding (i.e., $n_1 \approx n_2$ or $\Delta \ll 1$) so that the guided rays are paraxial, i.e., approximately parallel to the fiber axis. The longitudinal components of the electric and magnetic fields are then far weaker than the transverse components and

the guided waves are approximately transverse electromagnetic (TEM) in nature. The linear polarization in the x and y directions then form orthogonal states of polarization. The linearly polarized (l, m) mode is usually denoted as the LP_{lm} mode. The two polarizations of mode (l, m) travel with the same propagation constant and have the same spatial distribution.

For weakly guiding fibers the characteristic equation obtained using the procedure outlined earlier turns out to be approximately equivalent to the conditions that the scalar function $u(r)$ in (9.2-6) is continuous and has a continuous derivative at $r = a$. These two conditions are satisfied if

$$\frac{(k_T a)J_l'(k_T a)}{J_l(k_T a)} = \frac{(\gamma a)K_l'(\gamma a)}{K_l(\gamma a)}. \tag{9.2-11}$$

The derivatives J_l' and K_l' of the Bessel functions satisfy the identities

$$J_l'(x) = \pm J_{l\mp1}(x) \mp l\frac{J_l(x)}{x} \tag{9.2-12}$$

$$K_l'(x) = -K_{l\mp1}(x) \mp l\frac{K_l(x)}{x}. \tag{9.2-13}$$

Substituting these identities into (9.2-11) and using the normalized parameters $X = k_T a$ and $Y = \gamma a$ leads to the characteristic equation

$$\boxed{X\frac{J_{l\pm1}(X)}{J_l(X)} = \pm Y\frac{K_{l\pm1}(Y)}{K_l(Y)}, \quad Y = \sqrt{V^2 - X^2}.} \tag{9.2-14}$$

Characteristic Equation

Given V and l, the characteristic equation contains a single unknown variable X. Note that $J_{-l}(x) = (-1)^l J_l(x)$ and $K_{-l}(x) = K_l(x)$, so that the equation remains unchanged if l is replaced by $-l$.

The characteristic equation may be solved graphically by plotting its right- and left-hand sides (RHS and LHS, respectively) versus X and finding the intersections. As illustrated in Fig. 9.2-3 for $l = 0$, the LHS has multiple branches whereas the RHS decreases monotonically with increasing X until it vanishes at $X = V$ ($Y = 0$). There are therefore multiple intersections in the interval $0 < X \leq V$. Each intersection point corresponds to a fiber mode with a distinct value of X. These values are denoted X_{lm}, $m = 1, 2, \ldots, M_l$ in order of increasing X. Once the X_{lm} are found, (9.2-8), (9.2-4), and (9.2-6) allow us to determine the corresponding transverse propagation constants k_{Tlm}, the decay parameters γ_{lm}, the propagation constants β_{lm}, and the radial distribution functions $u_{lm}(r)$. The graph in Fig. 9.2-3 is similar in character to that in Fig. 8.2-2, which governs the modes of a planar dielectric waveguide.

Each mode has a distinct radial distribution. As examples, the two radial distributions $u(r)$ illustrated in Fig. 9.2-2 correspond to the LP_{01} mode ($l = 0$, $m = 1$) in a fiber with $V = 5$, and the LP_{34} mode ($l = 3$, $m = 4$) in a fiber with $V = 25$, respectively. Since the (l, m) and $(-l, m)$ modes have the same propagation constant, it is of interest to examine the spatial distribution of their equal-weight superposition. The complex amplitude of the sum is proportional to $u_{lm}(r)\cos l\phi\, \exp(-j\beta_{lm}z)$. The intensity, which is proportional to $u_{lm}^2(r)\cos^2 l\phi$, is illustrated in Fig. 9.2-4 for the LP_{01} and LP_{34} modes (the same modes for which $u(r)$ is displayed in Fig. 9.2-2).

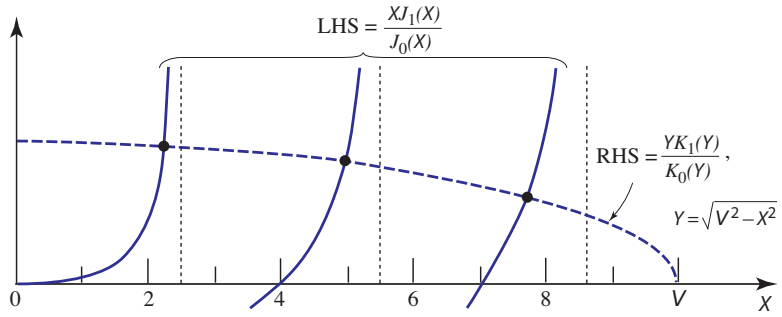

Figure 9.2-3 Graphical construction for solving the characteristic equation (9.2-14). The left- and right-hand sides are plotted as functions of X. The intersection points are the solutions. The LHS has multiple branches intersecting the abscissa at the roots of $J_{l\pm1}(X)$. The RHS intersects each branch once and meets the abscissa at $X = V$. The number of modes therefore equals the number of roots of $J_{l\pm1}(X)$ that are smaller than V. In this plot $l = 0$, $V = 10$, and either the $-$ or $+$ signs in (9.2-14) may be used.

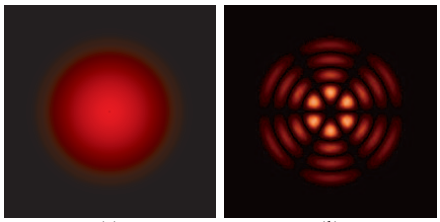

Figure 9.2-4 Intensity distributions of (a) the LP_{01} and (b) the LP_{34} modes in the transverse plane, assuming an azimuthal dependence of the form $\cos l\phi$. The distribution of the fundamental LP_{01} mode is similar to that of the Gaussian beam discussed in Chapter 3.

Mode Cutoff

It is evident from the graphical construction in Fig. 9.2-3 that as V increases, the number of intersections (modes) increases since the LHS of the characteristic equation (9.2-14) is independent of V, whereas the RHS moves to the right as V increases. Considering the minus signs in the characteristic equation, branches of the LHS intersect the abscissa when $J_{l-1}(X) = 0$. These roots are denoted x_{lm}, $m = 1, 2, \ldots$. The number of modes M_l is therefore equal to the number of roots of $J_{l-1}(X)$ that are smaller than V. The (l, m) mode is allowed if $V > x_{lm}$. The mode reaches its cutoff point when $V = x_{lm}$. As V decreases, the $(l, m-1)$ mode also reaches its cutoff point when a new root is reached, and so on. The smallest root of $J_{l-1}(X)$ is $x_{01} = 0$ for $l = 0$ and the next smallest is $x_{11} = 2.405$ for $l = 1$. The numerical values of some of these roots are provided in Table 9.2-1.

Table 9.2-1 Cutoff V parameter for low-order LP_{lm} modes.[a]

$l \backslash m$	1	2	3
0	0	3.832	7.016
1	2.405	5.520	8.654

[a] The cutoffs of the $l = 0$ modes occur at the roots of $J_{-1}(X) = -J_1(X)$. The $l = 1$ modes are cut off at the roots of $J_0(X)$, and so on.

When $V < 2.405$, all modes with the exception of the fundamental LP_{01} mode are cut off. The fiber then operates as a single-mode waveguide. The condition for single-

mode operation is therefore

$$\boxed{V < 2.405.} \qquad (9.2\text{-}15)$$
Single-Mode Condition

Since V is proportional to the optical frequency [see (9.2-10)], the cutoff condition for the fundamental mode provided in (9.2-15) yields a corresponding cutoff frequency:

$$\boxed{\nu_c = \omega_c/2\pi = \frac{1}{\text{NA}}\,\frac{c_o}{2.61a}\,.} \qquad (9.2\text{-}16)$$
Cutoff Frequency

By comparison, in accordance with (8.2-9), the cutoff frequency of the lowest-order mode in a dielectric slab waveguide of width d is $\nu_c = (1/\text{NA})(c_o/2d)$.

Number of Modes

A plot of the number of modes M_l as a function of V therefore takes the form of a staircase function that increases by unity at each of the roots x_{lm} of the Bessel function $J_{l-1}(X)$. A composite count of the total number of modes M (for all values of l), as a function of V, is provided in Fig. 9.2-5. Each root must be counted twice since, for each mode of azimuthal index $l > 0$, there is a corresponding mode $-l$ that is identical except for opposite polarity of the angle ϕ (corresponding to rays with helical trajectories of opposite senses), as can be seen by using the plus signs in the characteristic equation. Moreover, each mode has two states of polarization and must therefore be counted twice.

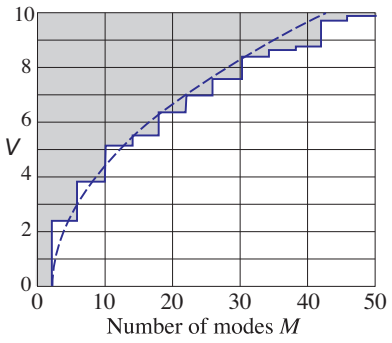

Figure 9.2-5 Total number of modes M versus the fiber parameter $V = 2\pi(a/\lambda_o)\text{NA}$. Included in the count are the two helical polarities for each mode with $l > 0$ and the two polarizations per mode. For $V < 2.405$, there is only a single mode, the fundamental LP_{01} mode with two polarizations. The dashed curve is the relation $M = 4V^2/\pi^2 + 2$, which provides an approximate formula for the number of modes when $V \gg 1$.

Number of Modes (Fibers with Large V Parameter)

For fibers with large V parameters, there are a large number of roots of $J_l(X)$ in the interval $0 < X < V$. Since $J_l(X) \approx (2/\pi X)^{1/2}\cos[X - (l + \frac{1}{2})\frac{\pi}{2}]$ when $X \gg 1$, its roots x_{lm} are approximately given by $x_{lm} = (l + \frac{1}{2})\frac{\pi}{2} + (2m - 1)\frac{\pi}{2}$. Thus, $x_{lm} = (l + 2m - \frac{1}{2})\frac{\pi}{2}$, so that when m is large the cutoff points of modes (l, m), which are the roots of $J_{l\pm1}(X)$, are

$$x_{lm} \approx \left(l + 2m - \tfrac{1}{2} \pm 1\right)\tfrac{\pi}{2} \approx (l + 2m)\tfrac{\pi}{2}, \qquad l = 0, 1, \ldots; \quad m \gg 1. \qquad (9.2\text{-}17)$$

For fixed l, these roots are spaced uniformly at a distance π, so that the number of roots M_l satisfies $(l + 2M_l)\frac{\pi}{2} = V$, from which $M_l \approx V/\pi - l/2$. Thus, M_l decreases linearly with increasing l, beginning with $M_l \approx V/\pi$ for $l = 0$ and ending at $M_l = 0$ when $l = l_{\max}$, where $l_{\max} = 2V/\pi$, as illustrated in Fig. 9.2-6. Thus, the total number of modes is $M \approx \sum_{l=0}^{l_{\max}} M_l = \sum_{l=0}^{l_{\max}} (V/\pi - l/2)$. Since the number of terms in this sum is assumed to be large, it may be readily evaluated by approximating it as the area of the unshaded triangle in Fig. 9.2-6: $M \approx \frac{1}{2}(2V/\pi)(V/\pi) = V^2/\pi^2$. Accommodating the two degrees of freedom for positive and negative l, and the two polarizations for each index (l, m), finally leads to

$$M \approx \frac{4}{\pi^2} V^2. \tag{9.2-18}$$

Number of Modes $(V \gg 1)$

Note that (9.2-18) is valid only for large V. This approximate number of modes is compared with the exact number, obtained from the characteristic equation, in Fig. 9.2-5.

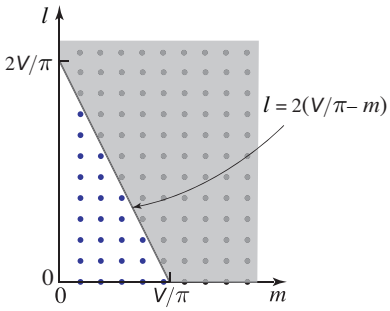

Figure 9.2-6 The indexes of guided modes extend from $m = 1$ to $m \approx V/\pi - l/2$ and from $l = 0$ to $l \approx 2V/\pi$, as displayed by the unshaded area.

The expression for the number of modes M for the circular waveguide given in (9.2-18), $M \approx (4a/\lambda_o)^2(\mathrm{NA})^2$, is analogous to the expression provided in (8.3-3) for the waveguide of rectangular cross section, $M \approx (\pi/4)(2d/\lambda_o)^2(\mathrm{NA})^2$.

EXAMPLE 9.2-1. ***Approximate Number of Modes.*** A silica fiber with $n_1 = 1.452$ and $\Delta = 0.01$ has a numerical aperture $\mathrm{NA} = \sqrt{n_1^2 - n_2^2} \approx n_1\sqrt{2\Delta} \approx 0.205$. If $\lambda_o = 0.85$ μm and the core radius $a = 25$ μm, then $V = 2\pi(a/\lambda_o)\mathrm{NA} \approx 37.9$. There are therefore approximately $M \approx 4V^2/\pi^2 \approx 585$ modes. If the cladding is stripped away so that the core is in direct contact with air, $n_2 = 1$ and $\mathrm{NA} = 1$, whereupon $V = 184.8$ and more than 13,800 modes are allowed.

Propagation Constants (Fibers with Large V Parameter)

As indicated earlier, the propagation constants can be determined by solving the characteristic equation (9.2-14) for the X_{lm} and using (9.2-4a) and (9.2-8) to obtain $\beta_{lm} = (n_1^2 k_o^2 - X_{lm}^2/a^2)^{1/2}$. A number of approximate formulas for X_{lm} applicable in certain limits are available in the literature, but there are no explicit exact formulas.

If $V \gg 1$, the crudest approximation is to assume that the X_{lm} are equal to the cutoff values x_{lm}. This is equivalent to assuming that the branches in Fig. 9.2-3 are

approximately vertical lines, so that $X_{lm} \approx x_{lm}$. Since $V \gg 1$, the majority of the roots would then be large so that the approximation in (9.2-17) may be used to obtain

$$\beta_{lm} \approx \sqrt{n_1^2 k_o^2 - (l+2m)^2 \frac{\pi^2}{4a^2}}\,. \tag{9.2-19}$$

Since

$$M \approx \frac{4}{\pi^2} V^2 = \frac{4}{\pi^2} (\mathrm{NA})^2 \cdot a^2 k_o^2 \approx \frac{4}{\pi^2} (2n_1^2 \Delta)\, k_o^2 a^2, \tag{9.2-20}$$

(9.2-19) and (9.2-20) yield

$$\beta_{lm} \approx n_1 k_o \sqrt{1 - 2\frac{(l+2m)^2}{M}\Delta}\,. \tag{9.2-21}$$

Because Δ is small, we may use the approximation $\sqrt{1+\delta} \approx 1 + \delta/2$ for $|\delta| \ll 1$ to obtain

$$\boxed{\beta_{lm} \approx n_1 k_o \left[1 - \frac{(l+2m)^2}{M}\Delta\right].} \tag{9.2-22}$$

Propagation Constants ($V \gg 1$)
$l = 0, 1, \ldots, \sqrt{M}$
$m = 1, 2, \ldots, \frac{1}{2}(\sqrt{M} - l)$

Since $l + 2m$ varies between 2 and $\approx 2V/\pi = \sqrt{M}$ (see Fig. 9.2-6), β_{lm} varies approximately between $n_1 k_o$ and $n_1 k_o(1-\Delta) \approx n_2 k_o$, as illustrated in Fig. 9.2-7.

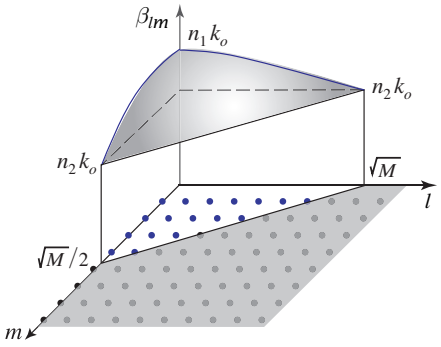

Figure 9.2-7 Approximate propagation constants β_{lm} of the modes of a fiber with large V parameter, as functions of the mode indexes l and m.

Group Velocities (Fibers with Large V Parameter)

To determine the group velocity, $v_{lm} = d\omega/d\beta_{lm}$, of the (l, m) mode we express β_{lm} as an explicit function of ω by substituting $n_1 k_o = \omega/c_1$ and $M = (4/\pi^2)(2n_1^2\Delta)k_o^2 a^2 = (8/\pi^2)a^2\omega^2\Delta/c_1^2$ into (9.2-22) and assume that c_1 and Δ are independent of ω. The derivative $d\omega/d\beta_{lm}$ provides

$$v_{lm} \approx c_1 \left[1 + \frac{(l+2m)^2}{M}\Delta\right]^{-1}. \tag{9.2-23}$$

Since $\Delta \ll 1$, the approximate expansion $(1+\delta)^{-1} \approx 1-\delta$ for $|\delta| \ll 1$, then leads to

$$v_{lm} \approx c_1 \left[1 - \frac{(l+2m)^2}{M}\,\Delta\right]. \qquad \text{(9.2-24)}$$

Group Velocities ($V \gg 1$)

Because the minimum and maximum values of $(l+2m)$ are 2 and $\sqrt{M}$, respectively, and since $M \gg 1$, the group velocity varies approximately between c_1 and $c_1(1-\Delta) = c_1(n_2/n_1)$. Thus, the group velocities of the low-order modes are approximately equal to the phase velocity of the core material, whereas those of the high-order modes are smaller.

The fractional group-velocity change between the fastest and the slowest mode is roughly equal to Δ, the fractional refractive index change of the fiber. Fibers with large Δ, although endowed with a large NA and therefore large light-gathering capacity, also have a large number of modes, large modal dispersion, and consequently high pulse-spreading rates. These effects are particularly severe if the cladding is removed altogether.

B. Single-Mode Fibers

As discussed earlier, a fiber with core radius a and numerical aperture NA operates as a single-mode fiber in the fundamental LP_{01} mode if $V = 2\pi(a/\lambda_o)\mathrm{NA} < 2.405$. Single-mode operation is therefore achieved via a small core diameter and small numerical aperture (in which case n_2 is close to n_1), or by operating at a sufficiently low optical frequency [below the cutoff frequency $\nu_c = (1/\mathrm{NA})(c_o/2.61a)$].

The fundamental mode has a bell-shaped spatial distribution similar to the Gaussian [see Fig. 9.2-2 for $l = 0$ and 9.2-4(a)]. It provides the highest confinement of light power within the core.

EXAMPLE 9.2-2. ***Single-Mode Operation.*** A silica-glass fiber with $n_1 = 1.447$ and $\Delta = 0.01$ ($\mathrm{NA} = 0.205$) operates at $\lambda_o = 1.3$ μm as a single-mode fiber if $V = 2\pi(a/\lambda_o)\mathrm{NA} < 2.405$, i.e., if the core diameter $2a < 4.86$ μm. If Δ is reduced to 0.0025, single-mode operation is maintained for a diameter $2a < 9.72$ μm.

The dependence of the effective refractive index $n = \beta/k_o$ on the V parameter for the fundamental mode is shown in Fig. 9.2-8(a), and the corresponding dispersion relation (ω versus β) is illustrated in Fig. 9.2-8(b). As the V parameter increases, i.e., the frequency increases or the fiber diameter increases, the effective refractive index n increases from n_2 to n_1. This is expected since the mode is more confined in the core at shorter wavelengths.

There are numerous advantages of using single-mode fibers in lightwave communication systems. As explained earlier, the modes of a multimode fiber travel at different group velocities so that a short-duration pulse of multimode light suffers a range of delays and therefore spreads in time. Quantitative measures of modal dispersion are examined in Sec. 9.3B. In a single-mode fiber, on the other hand, there is only one mode with one group velocity, so that a short pulse of light arrives without delay distortion. As explained in Sec. 9.3B, pulse spreading in single-mode fibers does result from other dispersive mechanisms, but these are significantly smaller than modal dispersion.

Moreover, as shown in Sec. 9.3A, the rate of power attenuation is lower in a single-mode fiber than in a multimode fiber. This, together with the smaller rate of pulse

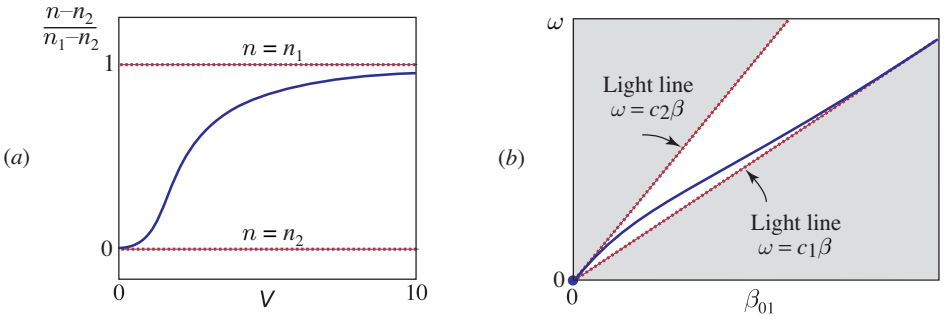

Figure 9.2-8 Schematic illustrations of the propagation characteristics of the fundamental LP_{01} mode. (a) Effective refractive index $n = \beta/k_o$ as a function of the V parameter. (b) Dispersion relation (ω versus β_{01}).

spreading, permits substantially higher data rates to be transmitted over single-mode fibers than over multimode fibers. This topic is considered further in Chapters 22 and 24.

Another difficulty with multimode fibers stems from the random interference of the modes. As a result of uncontrollable imperfections, strains, and temperature fluctuations, each mode undergoes a random phase shift so that the sum of the complex amplitudes of the modes exhibits an intensity that is random in time and space. This randomness is known as **modal noise** or **speckle**. This effect is similar to the fading of radio signals resulting from multiple-path transmission. In a single-mode fiber there is only one path and therefore no modal noise.

Polarization-Maintaining Fibers

In a fiber with circular cross section, each mode has two independent states of polarization with the same propagation constant. Thus, the fundamental LP_{01} mode in a single-mode weakly guiding fiber may be polarized in the x or y direction; the two orthogonal polarizations have the same propagation constant and the same group velocity.

In principle, there should be no exchange of power between the two polarization components. If the power of the light source is delivered exclusively into one polarization, the power should remain in that polarization. In practice, however, slight random imperfections and uncontrollable strains in the fiber result in random power transfer between the two polarizations. Such coupling is facilitated because the two polarizations have the same propagation constant and their phases are therefore matched. Thus, linearly polarized light at the fiber input is generally transformed into elliptically polarized light at the fiber output. In spite of the fact that the total optical power remains fixed (see Fig. 9.2-9), the ellipticity of the received light fluctuates randomly with time as a result of fluctuations in the material strain and temperature, and of the source wavelength. The randomization of the power division between the two polarization components poses no difficulty if the object is solely to transmit light power, provided that the total power is collected.

However, in many areas where fiber optics is used, e.g., integrated-optic devices, optical sensors based on interferometric techniques, and coherent optical communications, the fiber must transmit the complex amplitude (magnitude and phase) of a specific polarization. Polarization-maintaining fibers are required for such applications. To construct a polarization-maintaining fiber, the circular symmetry of the conventional fiber must be abandoned, such as by using fibers with elliptical cross section or stress-induced anisotropy of the refractive index. This eliminates the polarization degeneracy, thereby making the propagation constants of the two polarizations different. The introduction of such phase mismatch serves to reduce the coupling efficiency.

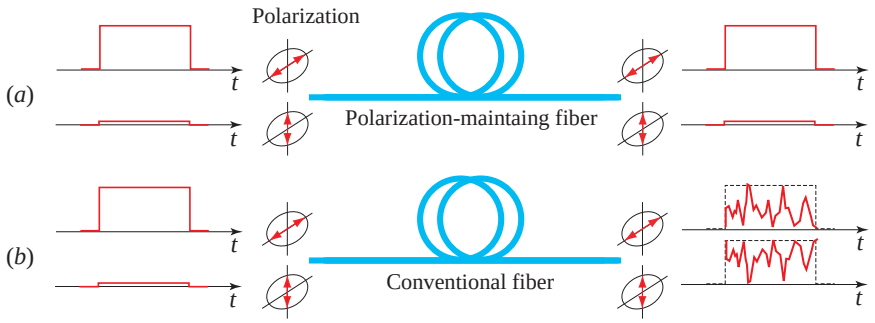

Figure 9.2-9 (a) Ideal polarization-maintaining fiber. (b) Random transfer of power between two polarizations.

*C. Quasi-Plane Waves in Step- and Graded-Index Fibers

The modes of the graded-index fiber are determined by writing the Helmholtz equation (9.2-1) with $n = n(r)$, solving for the spatial distributions of the field components, and using Maxwell's equations and the boundary conditions to obtain the characteristic equation, as was done for the step-index case. This procedure is difficult, in general.

In this section we use instead an approximate approach based on picturing the field distribution as a quasi-plane wave traveling within the core, approximately along the trajectory of the optical ray. A quasi-plane wave is a wave that is locally identical to a plane wave, but changes its direction and amplitude slowly as it travels. This approach permits us to maintain the simplicity of rays optics but at the same time retain the phase associated with the wave, so that the self-consistency condition to determine the propagation constants of the guided modes can be used (as was done for the planar dielectric waveguide in Sec. 8.2). This approximate technique, called the WKB (Wentzel–Kramers–Brillouin) method, is applicable only to fibers with a large number of modes (large V parameter).

Quasi-Plane Waves

Consider a solution of the Helmholtz equation (9.2-1) that takes the form of a quasi-plane wave (see Sec. 2.3)

$$U(\mathbf{r}) = \mathsf{a}(\mathbf{r}) \exp\left[-jk_o \mathsf{S}(\mathbf{r})\right], \tag{9.2-25}$$

where $\mathsf{a}(\mathbf{r})$ and $\mathsf{S}(\mathbf{r})$ are real functions of position that are slowly varying in comparison with the wavelength $\lambda_o = 2\pi/k_o$. It is known from (2.3-4) that $\mathsf{S}(\mathbf{r})$ approximately satisfies the eikonal equation $|\nabla \mathsf{S}|^2 \approx n^2$, and that the rays travel in the direction of the gradient $\nabla \mathsf{S}$. If we take $k_o \mathsf{S}(\mathbf{r}) = k_o \mathsf{s}(r) + l\phi + \beta z$, where $\mathsf{s}(r)$ is a slowly varying function of r, the eikonal equation gives

$$\left(k_o \frac{d\mathsf{s}}{dr}\right)^2 + \beta^2 + \frac{l^2}{r^2} = n^2(r)\, k_o^2. \tag{9.2-26}$$

The local spatial frequency of the wave in the radial direction is the partial derivative of the phase $k_o \mathsf{S}(\mathbf{r})$ with respect to r,

$$k_r = k_o \frac{d\mathsf{s}}{dr}, \tag{9.2-27}$$

so that (9.2-25) becomes

$$U(r) = \mathfrak{a}(r)\, \exp\left(-j \int_0^r k_r\, dr\right) e^{-jl\phi} e^{-j\beta z} \tag{9.2-28}$$

Quasi-Plane Wave

and (9.2-26) gives

$$k_r^2 = n^2(r)\, k_o^2 - \beta^2 - \frac{l^2}{r^2}. \tag{9.2-29}$$

Defining $k_\phi = l/r$ so that $\exp(-jl\phi) = \exp(-jk_\phi r\phi)$, and $k_z = \beta$, (9.2-29) yields $k_r^2 + k_\phi^2 + k_z^2 = n^2(r)\, k_o^2$. The quasi-plane wave therefore has a local wavevector $\mathbf{k}$ with magnitude $n(r)k_o$ and cylindrical-coordinate components (k_r, k_ϕ, k_z). Since $n(r)$ and k_ϕ are functions of r, k_r is also generally position dependent. The direction of $\mathbf{k}$ changes slowly with r (see Fig. 9.2-10), following a helical trajectory similar to that of the skewed ray shown earlier in Fig. 9.1-6(b).

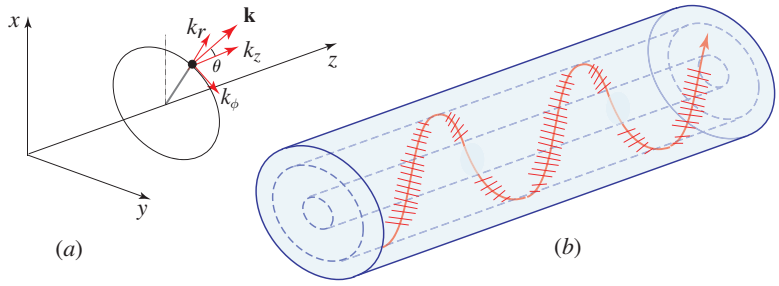

Figure 9.2-10 (a) The wavevector $\mathbf{k} = (k_r, k_\phi, k_z)$ in a cylindrical coordinate system. (b) Quasi-plane wave following the direction of a ray.

To establish the region of the core within which the wave is bound, we determine the values of r for which k_r is real, or $k_r^2 > 0$. For a given l and β we plot $k_r^2 = [n^2(r)\, k_o^2 - l^2/r^2 - \beta^2]$ as a function of r. The term $n^2(r)\, k_o^2$ is first plotted as a function of r [thick solid curve in Fig. 9.2-11(a)]. The term l^2/r^2 is then subtracted, yielding the dashed curve. The value of β^2 is marked by the thin solid vertical line. It follows that k_r^2 is represented by the difference between the dashed curve and the thin solid line, i.e., by the shaded area. Regions where k_r^2 is positive and negative are indicated by $+$ and $-$ signs, respectively.

For the step-index fiber, we have $n(r) = n_1$ for $r < a$, and $n(r) = n_2$ for $r > a$. In this case the quasi-plane wave is guided in the core by reflecting from the core–cladding boundary at $r = a$. As illustrated in Fig. 9.2-11(a), the region of confinement is then $r_l < r < a$, where

$$n_1^2 k_o^2 - \frac{l^2}{r_l^2} - \beta^2 = 0. \tag{9.2-30}$$

The wave bounces back and forth helically like the skewed ray illustrated in Fig. 9.1-2. In the cladding $(r > a)$, and near the center of the core $(r < r_l)$, k_r^2 is negative so that

k_r is imaginary; the wave therefore decays exponentially in these regions. Note that r_l depends on β. For large β (or large l), r_l is large so that the wave is confined to a thin cylindrical shell near the boundary of the core.

For the graded-index fiber illustrated in Fig. 9.2-11(b), k_r is real in the region $r_l < r < R_l$, where r_l and R_l are the roots of the equation

$$n^2(r)\,k_o^2 - \frac{l^2}{r^2} - \beta^2 = 0. \tag{9.2-31}$$

It follows that the wave is essentially confined within a cylindrical shell of radii r_l and R_l, just as for the helical ray trajectory shown in Fig. 9.1-6(b).

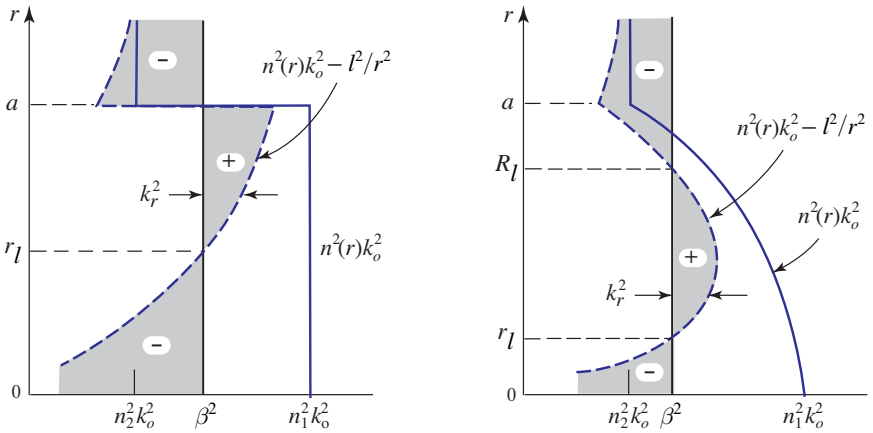

(a) Step-index (b) Graded-index

Figure 9.2-11 Dependence of $n^2(r)\,k_o^2$, $n^2(r)\,k_o^2 - l^2/r^2$, and $k_r^2 = n^2(r)\,k_o^2 - l^2/r^2 - \beta^2$ on the position r. At any r, k_r^2 is the width of the shaded area with the $+$ and $-$ signs denoting positive and negative values of k_r^2, respectively. (a) Step-index fiber: k_r^2 is positive in the region $r_l < r < a$. (b) Graded-index fiber: k_r^2 is positive in the region $r_l < r < R_l$.

Modes

The modes of the fiber are determined by imposing the self-consistency condition that the wave reproduce itself after one helical period of travel between r_l and R_l and back. The azimuthal path length corresponding to an angle 2π must correspond to a multiple of 2π phase shift, i.e., $k_\phi 2\pi r = 2\pi l$; $l = 0, \pm1, \pm2, \ldots$. This condition is evidently satisfied since $k_\phi = l/r$. Furthermore, the radial round-trip path length must correspond to a phase shift equal to an integer multiple of 2π:

$$2\int_{r_l}^{R_l} k_r\,dr = 2\pi m, \qquad m = 1, 2, \ldots, M_l, \tag{9.2-32}$$

where $R_l = a$ for the step-index fiber. This condition, which is analogous to the self-consistency condition (8.2-2) for planar waveguides, provides the characteristic equation from which the propagation constants β_{lm} of the modes are determined. These values are indicated schematically in Fig. 9.2-12; the mode $m = 1$ has the largest value of β (approximately n_1k_o) whereas $m = M_l$ has the smallest value (approximately n_2k_o).

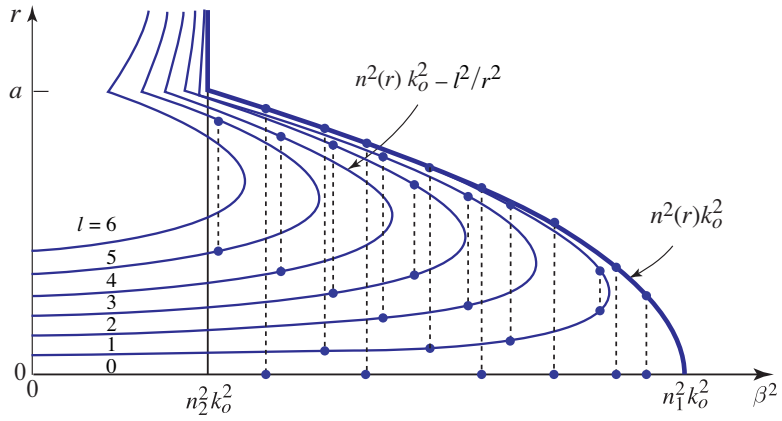

Figure 9.2-12 The propagation constants and confinement regions of the fiber modes. Each curve corresponds to an index l, which stretches from 0 to 6 in this plot. Each mode (corresponding to a certain value of m) is marked schematically by two dots connected by a dashed vertical line. The ordinates of the dots mark the radii r_l and R_l of the cylindrical shell within which the mode is confined. Values on the abscissa are the squared propagation constants of the modes, β^2.

Number of Modes

The total number of modes can be determined by adding the number of modes M_l for $l = 0, 1, \ldots, l_{\max}$. We consider this computation using a different procedure, however. We first determine the number q_β of modes with propagation constants greater than a given value β. For each l, the number of modes $M_l(\beta)$ with propagation constant greater than β is the number of multiples of 2π the integral in (9.2-32) yields, i.e.,

$$M_l(\beta) = \frac{1}{\pi}\int_{r_l}^{R_l} k_r\, dr = \frac{1}{\pi}\int_{r_l}^{R_l} \sqrt{n^2(r)k_o^2 - \frac{l^2}{r^2} - \beta^2}\, dr, \tag{9.2-33}$$

where r_l and R_l are the radii of confinement corresponding to the propagation constant β as given by (9.2-31). Clearly, r_l and R_l depend on β, and $R_l = a$ for the step-index fiber.

The total number of modes with propagation constant greater than β is therefore

$$q_\beta = 4\sum_{l=0}^{l_{\max}(\beta)} M_l(\beta), \tag{9.2-34}$$

where $l_{\max}(\beta)$ is the maximum value of l that yields a bound mode with propagation constants greater than β, i.e., for which the peak value of the function $n^2(r)\,k_o^2 - l^2/r^2$ is greater than β^2. The grand total mode count M is q_β for $\beta = n_2k_o$. The factor of 4 in (9.2-34) accommodates the two possible polarizations and the two possible polarities of the angle ϕ, corresponding to positive and negative helical trajectories for each (l, m). If the number of modes is sufficiently large, we can replace the summation in (9.2-34) by an integral, whereupon

$$q_\beta \approx 4\int_0^{l_{\max}(\beta)} M_l(\beta)\, dl. \tag{9.2-35}$$

For fibers with power-law refractive-index profiles, we insert (9.1-4) into (9.2-33),

and thence into (9.2-35). Evaluation of the integral then yields

$$q_\beta \approx M \left[\frac{1 - (\beta/n_1 k_o)^2}{2\Delta} \right]^{\frac{p+2}{p}} \tag{9.2-36}$$

with

$$M \approx \frac{p}{p+2} n_1^2 k_o^2 a^2 \Delta = \frac{p}{p+2} \frac{V^2}{2}, \tag{9.2-37}$$

where $\Delta = (n_1 - n_2)/n_1$ and $V = 2\pi(a/\lambda_o)\text{NA}$ is the fiber V parameter. Since $q_\beta \approx M$ at $\beta = n_2 k_o$, M is indeed the total number of modes.

For step-index fibers $(p \to \infty)$, (9.2-36) and (9.2-37) become

$$q_\beta \approx M \left[\frac{1 - (\beta/n_1 k_o)^2}{2\Delta} \right] \tag{9.2-38}$$

and

$$\boxed{M \approx \frac{1}{2} V^2,} \tag{9.2-39}$$

Number of Modes (Step-Index)

respectively. This expression for M is nearly the same as that set forth in (9.2-18), $M \approx 4V^2/\pi^2 \approx 0.41V^2$, which was obtained in Sec. 9.2 using a different approximation.

Propagation Constants

The propagation constant β_q for mode q is obtained by inverting (9.2-36),

$$\beta_q \approx n_1 k_o \sqrt{1 - 2\left(\frac{q}{M}\right)^{p/(p+2)} \Delta}, \qquad q = 1, 2, \ldots, M, \tag{9.2-40}$$

where the index q_β has been replaced by q, and β replaced by β_q. Since $\Delta \ll 1$, the approximation $\sqrt{1+\delta} \approx 1 + \frac{1}{2}\delta$ (applicable for $|\delta| \ll 1$) can be applied to (9.2-40), yielding

$$\boxed{\beta_q \approx n_1 k_o \left[1 - \left(\frac{q}{M}\right)^{p/(p+2)} \Delta \right].} \tag{9.2-41}$$

Propagation Constants

The propagation constant β_q therefore decreases from $\approx n_1 k_o$ (for $q = 1$) to $n_2 k_o$ (for $q = M$), as illustrated in Fig. 9.2-13.

For the step-index fiber $(p \to \infty)$, (9.2-40) reduces to

$$\boxed{\beta_q \approx n_1 k_o \left(1 - \frac{q}{M} \Delta \right).} \tag{9.2-42}$$

Propagation Constants (Step-Index Fiber)

This expression is identical to (9.2-22) if the index $q = 1, 2, \ldots, M$ is replaced by $(l + 2m)^2$, with $l = 0, 1, \ldots, \sqrt{M}$; $m = 1, 2, \ldots, \frac{1}{2}(\sqrt{M} - l)$.

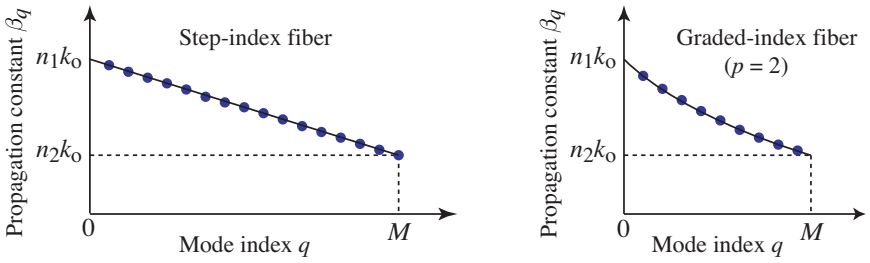

Figure 9.2-13 Dependence of the propagation constants β_q on the mode index $q = 1, 2, \ldots, M$ for a step-index fiber ($p \to \infty$) and for an optimal graded-index fiber ($p = 2$).

Group Velocities

To determine the group velocity $v_q = d\omega/d\beta_q$, we write β_q as a function of ω by substituting (9.2-37) into (9.2-41), substituting $n_1 k_o = \omega/c_1$ into the result, and evaluating $v_q = (d\beta_q/d\omega)^{-1}$. With the help of the approximation $(1+\delta)^{-1} \approx 1 - \delta$ (valid for $|\delta| \ll 1$), and assuming that c_1 and Δ are independent of ω (i.e., ignoring material dispersion), we obtain

$$v_q \approx c_1 \left[1 - \frac{p-2}{p+2}\left(\frac{q}{M}\right)^{p/(p+2)} \Delta\right]. \tag{9.2-43}$$

Group Velocities

For the step-index fiber $(p \to \infty)$, (9.2-43) yields

$$v_q \approx c_1 \left(1 - \frac{q}{M}\Delta\right), \tag{9.2-44}$$

which reproduces (9.2-24). The group velocity thus varies from approximately c_1 to $c_1(1-\Delta)$, as illustrated in Fig. 9.2-14(a).

Optimal Index Profile

Equation (9.2-43) indicates that the grade profile parameter $p = 2$ yields a group velocity $v_q \approx c_1$ for all q, so that all modes travel at approximately the same velocity c_1. This highlights the advantage of the graded-index fiber for multimode transmission.

To determine the group velocity with better accuracy, we return to the derivation of v_q from (9.2-40) for $p = 2$. Carrying the Taylor-series expansion to three terms instead of two, i.e., $\sqrt{1+\delta} \approx 1 + \frac{1}{2}\delta - \frac{1}{8}\delta^2$, gives rise to

$$v_q \approx c_1 \left(1 - \frac{q}{M}\frac{\Delta^2}{2}\right). \tag{9.2-45}$$

Group Velocities (Graded-Index, $p = 2$)

Thus, the group velocities vary from approximately c_1 at $q = 1$ to approximately $c_1(1 - \Delta^2/2)$ at $q = M$. Comparison with the results for the step-index fiber is provided in Fig. 9.2-14. The group-velocity difference for the parabolically graded fiber is $\Delta^2/2$, which is substantially smaller than the group-velocity difference Δ for the step-index fiber. Under ideal conditions, the graded-index fiber therefore reduces the group-velocity difference by a factor $\Delta/2$, thus realizing its intended purpose of

equalizing the modal velocities. However, since the analysis leading to (9.2-45) is based on a number of approximations, this improvement factor is only a rough estimate — indeed it is not fully attained in practice.

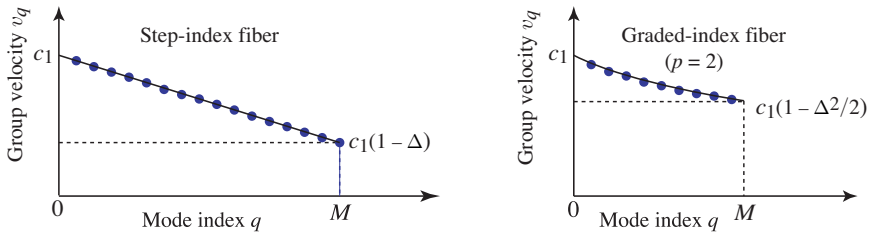

Figure 9.2-14 Group velocities v_q of the modes of a step-index fiber $(p \to \infty)$ and an optimal graded-index fiber $(p = 2)$.

The number of modes M in a graded-index fiber with grade profile parameter p is specified by (9.2-37). For $p = 2$, this becomes

$$M \approx \frac{1}{4}V^2. \tag{9.2-46}$$

Number of Modes (Graded-Index, $p = 2$)

Comparing this with the result for the step-index fiber provided in (9.2-39), $M \approx V^2/2$, reveals that the number of modes in an optimal graded-index fiber is roughly half that in a step-index fiber with the same parameters n_1, n_2, and a.

9.3 ATTENUATION AND DISPERSION

Attenuation and dispersion limit the performance of the optical-fiber medium as a data-transmission channel. Attenuation, associated with losses of various kinds, limits the magnitude of the optical power transmitted. Dispersion, which is responsible for the temporal spread of optical pulses, limits the rate at which such data-carrying pulses may be transmitted.

A. Attenuation

Attenuation Coefficient

The power of a light beam traveling through an optical fiber decreases exponentially with distance as a result of absorption and scattering. The associated attenuation coefficient is conventionally defined in units of decibels per kilometer (dB/km) and is denoted by the symbol α,

$$\alpha = \frac{1}{L}\, 10 \log_{10} \frac{1}{\mathcal{T}}, \tag{9.3-1}$$

where $\mathcal{T} = P(L)/P(0)$ is the power transmission ratio (ratio of transmitted to incident power) for a fiber of length L km. The conversion of a ratio to dB units is illustrated in

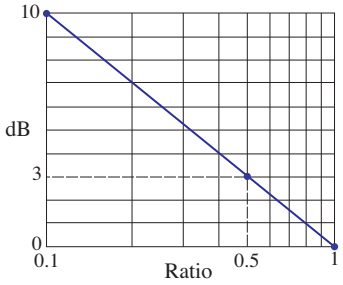

Figure 9.3-1 The dB value of a ratio. For example, 3 dB is equivalent to a ratio of 0.5; 10 dB corresponds to $\mathcal{T} = 0.1$; and 20 dB corresponds to $\mathcal{T} = 0.01$.

Fig. 9.3-1. An attenuation of 3 dB/km, for example, corresponds to a power transmission of $\mathcal{T} = 0.5$ through a fiber of length $L = 1$ km.

For light traveling through a cascade of lossy systems, the overall transmission ratio is the *product* of the constituent transmission ratios. By virtue of the logarithm in (9.3-1), the overall loss in dB therefore becomes the *sum* of the constituent dB losses. For a propagation distance of z km, the loss is αz dB. The associated power transmission ratio, which is obtained by inverting (9.3-1), is then

$$\frac{P(z)}{P(0)} = 10^{-\alpha z/10} \approx e^{-0.23\,\alpha z}, \qquad \alpha \text{ in dB/km}. \tag{9.3-2}$$

Equation (9.3-2) applies when the quantity α is specified in units of dB/km. However, that if the attenuation coefficient is specified in units of km^{-1}, rather than in units of dB/km, then

$$P(z)/P(0) = e^{-\alpha z}, \qquad \alpha \text{ in km}^{-1}, \tag{9.3-3}$$

where $\alpha \approx 0.23\,\alpha$. The attenuation coefficient α is usually specified in units of cm^{-1} for components other than optical fibers, in which case the power attenuation is described by (9.3-3) with z in cm.

Absorption

The attenuation coefficient α of fused silica (SiO_2) is strongly dependent on wavelength, as illustrated in Fig. 9.3-2. This material has two strong absorption bands: a mid-infrared absorption band resulting from vibrational transitions and an ultraviolet absorption band arising from electronic and molecular transitions. The tails of these bands form a window in the near infrared region of the spectrum in which there is little intrinsic absorption.

Scattering

Rayleigh scattering is another intrinsic effect that contributes to the attenuation of light in glass. The random localized variations of the molecular positions in the glass itself create random inhomogeneities in the refractive index that act as tiny scattering centers. The amplitude of the scattered field is proportional to ω^2, where ω is the angular frequency of the light.† The scattered intensity is therefore proportional to ω^4, or to $1/\lambda_o^4$, so that short wavelengths are scattered more than long wavelengths. Blue light is therefore scattered more than red (a similar effect, the scattering of sunlight from atmospheric molecules, is the reason the sky appears blue).

† The scattering medium creates a polarization density $\mathcal{P}$, which corresponds to a source of radiation proportional to $d^2\mathcal{P}/dt^2 = -\omega^2\mathcal{P}$; see (5.2-25).

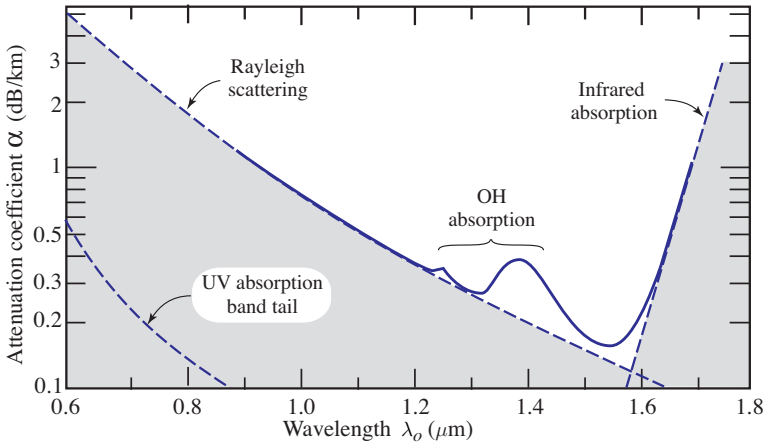

Figure 9.3-2 Attenuation coefficient α of silica glass versus wavelength λ_o. There is a local minimum at $1.3\ \mu\text{m}$ ($\alpha \approx 0.3\ \text{dB/km}$) and an absolute minimum at $1.55\ \mu\text{m}$ ($\alpha \approx 0.15\ \text{dB/km}$).

The functional form of Rayleigh scattering, which decreases with wavelength as $1/\lambda_o^4$, is known as **Rayleigh's inverse fourth-power law**. In the visible region of the spectrum, Rayleigh scattering is a more significant source of loss than is the tail of the ultraviolet absorption band, as shown in Fig. 9.3-2. However, Rayleigh loss becomes negligible in comparison with infrared absorption for wavelengths greater than $1.6\ \mu\text{m}$.

We conclude that the transparent window in silica glass is bounded by Rayleigh scattering on the short-wavelength side and by infrared absorption on the long-wavelength side (indicated by the dashed curves in Fig. 9.3-2). Lightwave communication systems are deliberately designed to operate in this window.

Extrinsic Effects

Aside from these intrinsic effects there are extrinsic absorption bands that result from the presence of impurities, principally metallic ions and OH radicals associated with water vapor dissolved in the glass. Most metal impurities can be readily removed but OH impurities are somewhat more difficult to eliminate. Only recently have specialty fibers with significantly reduced OH absorption become available. In general, wavelengths at which glass fibers are used for lightwave communication are selected to avoid the OH absorption bands.

Light-scattering losses may also be accentuated when dopants are added, as they often are for purposes of index grading. The attenuation coefficient for guided light in glass fibers depends on the absorption and scattering in the core and cladding materials. Each mode has a different penetration depth into the cladding, causing the rays to travel different effective distances and rendering the attenuation coefficient mode dependent. It is generally higher for higher-order modes. Single-mode fibers therefore typically have smaller attenuation coefficients than multimode fibers (Fig. 9.3-3). Losses are also introduced by small random variations in the geometry of the fiber and by bends.

Alternates to Silica Glass

A number of materials other than silica glass are being examined for potential use in mid-infrared optical fiber systems. These include heavy-metal fluoride glasses, heavy-metal germanate glasses, and chalcogenide glasses. The infrared absorption band is located further into the infrared for these materials than it is for silica glass so that longer-wavelength operation, with its attendant reduced Rayleigh scattering (which

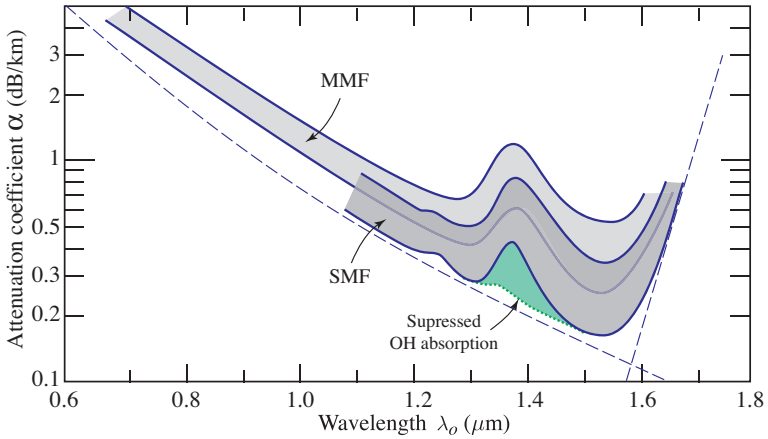

Figure 9.3-3 Ranges of attenuation coefficients for silica-glass single-mode fibers (SMF) and multimode fibers (MMF).

decreases as $1/\lambda_o^4$), is possible. In particular, the optical attenuation for heavy-metal fluoride glass fibers is predicted to be about 10 times smaller than for silica fibers, reaching a minimum of ≈ 0.01 dB/km at $\lambda_o \approx 2.5$ μm. However, extrinsic loss mechanisms currently dominate fiber loss and these materials are generally far less durable than silica glass. Although quantum-cascade lasers offer room-temperature operation in the mid infrared, high-efficiency photodetectors are generally not available in this spectral region.

B. Dispersion

When a short pulse of light travels through an optical fiber, its power is "dispersed" in time so that the pulse spreads into a wider time interval. There are five principal sources of dispersion in optical fibers:

- Modal dispersion
- Material dispersion
- Waveguide dispersion
- Polarization-mode dispersion
- Nonlinear dispersion

The combined contributions of these effects to the spread of pulses in time are not necessarily additive, as will be subsequently shown.

Modal Dispersion

Modal dispersion occurs in multimode fibers as a result of the differences in the group velocities of the various modes. A single impulse of light entering an M-mode fiber at $z = 0$ spreads into M pulses whose differential delay increases as a function of z. For a fiber of length L, the time delays engendered by the different velocities are $\tau_q = L/v_q$, $q = 1, \ldots, M$, where v_q is the group velocity of mode q. If $v_{\min}$ and $v_{\max}$ are the smallest and largest group velocities, respectively, the received pulse spreads over a time interval $L/v_{\min} - L/v_{\max}$. Since the modes are usually not excited equally, the overall shape of the received pulse generally has a smooth envelope, as illustrated in Fig. 9.3-4. An estimate of the overall pulse duration (assuming a triangular envelope and using the FWHM definition of the width) is $\sigma_\tau = \frac{1}{2}(L/v_{\min} - L/v_{\max})$, which represents the modal-dispersion response time of the fiber.

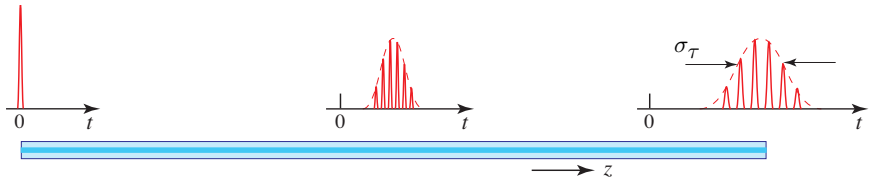

Figure 9.3-4 Pulse spreading caused by modal dispersion.

In a step-index fiber with a large number of modes, $v_{\min} \approx c_1(1-\Delta)$ and $v_{\max} \approx c_1$ [see Sec. 9.2C and Fig. 9.2-14(a)]. Since $(1-\Delta)^{-1} \approx 1+\Delta$ for $\Delta \ll 1$, the response time turns out to be a fraction $\Delta/2$ of the delay time L/c_1:

$$\sigma_\tau \approx \frac{L}{c_1} \cdot \frac{\Delta}{2}. \tag{9.3-4}$$

Response Time (Multimode Step-Index)

Modal dispersion is far smaller in graded-index (GRIN) fibers than in step-index fibers since the group velocities are equalized and the differences between the delay times of the modes, $\tau_q = L/v_q$, are reduced. It was shown in Sec. 9.2C and in Fig. 9.2-14(b) that a graded-index fiber with an optimal index profile and a large number of modes has $v_{\max} \approx c_1$ and $v_{\min} \approx c_1(1-\Delta^2/2)$. The response time in this case is therefore a factor of $\Delta/2$ smaller than that in a step-index fiber:

$$\sigma_\tau \approx \frac{L}{c_1} \cdot \frac{\Delta^2}{4}. \tag{9.3-5}$$

Response Time (Graded-Index)

EXAMPLE 9.3-1. ***Multimode Pulse Broadening Rate.*** In a step-index fiber with $\Delta = 0.01$ and $n = 1.46$, pulses spread at a rate of approximately $\sigma_\tau/L = \Delta/2c_1 = n_1\Delta/2c_o \approx 24$ ns/km. In a 100-km fiber, therefore, an impulse spreads to a width of ≈ 2.4 μs. If the same fiber is optimally index graded, the pulse broadening rate is approximately $n_1\Delta^2/4c_o \approx 122$ ps/km, a substantial reduction.

The pulse broadening arising from modal dispersion is proportional to the fiber length L in both step-index and GRIN fibers. Because of mode coupling, however, this dependence does not necessarily apply for fibers longer than a certain critical length. Coupling occurs between modes that have approximately the same propagation constants as a result of small imperfections in the fiber, such as random irregularities at its surface or inhomogeneities in its refractive index. This permits optical power to be exchanged between the modes. Under certain conditions, the response time σ_τ of mode-coupled fibers is proportional to L for small fiber lengths and to $\sqrt{L}$ when a critical length is exceeded, whereupon the pulses are broadened at a reduced rate.[†]

Material Dispersion

Glass is a dispersive medium, i.e., its refractive index is a function of wavelength. As discussed in Sec. 5.6, an optical pulse travels in a dispersive medium of refractive

[†] See, e.g., J. E. Midwinter, *Optical Fibers for Transmission*, Wiley, 1979; Krieger, reissued 1992.

index n with a group velocity $v = c_o/N$, where $N = n - \lambda_o\, dn/d\lambda_o$. Since the pulse is a wavepacket, comprising a collection of components of different wavelengths, each traveling at a different group velocity, its width spreads. The temporal duration of an optical impulse of spectral width σ_λ (nm), after traveling a distance L through a dispersive material, is $\sigma_\tau = |(d/d\lambda_o)(L/v)|\sigma_\lambda = |(d/d\lambda_o)(LN/c_o)|\sigma_\lambda$. This leads to a response time [see (5.6-2), (5.6-7), and (5.6-8)]

$$\boxed{\sigma_\tau = |D_\lambda|\sigma_\lambda L,} \qquad \begin{matrix}(9.3\text{-}6)\\ \text{Response Time}\\ \text{(Material Dispersion)}\end{matrix}$$

where the material dispersion coefficient D_λ is

$$D_\lambda = -\frac{\lambda_o}{c_o}\frac{d^2 n}{d\lambda_o^2}\,. \qquad (9.3\text{-}7)$$

The response time increases linearly with the distance L. Usually, L is measured in km, σ_τ in ps, and σ_λ in nm, so that D_λ has units of ps/km-nm. This type of dispersion is called **material dispersion**.

The wavelength dependence of the dispersion coefficient D_λ for a silica-glass fiber is displayed in Fig. 9.3-5. At wavelengths shorter than $1.3\ \mu$m the dispersion coefficient is negative, so that wavepackets of long wavelength travel faster than those of short wavelength. At a wavelength $\lambda_o = 0.87\ \mu$m, for example, the dispersion coefficient D_λ is approximately -80 ps/km-nm. At $\lambda_o = 1.55\ \mu$m, on the other hand, $D_\lambda \approx +17$ ps/km-nm. At $\lambda_o \approx 1.312\ \mu$m the dispersion coefficient vanishes, so that σ_τ in (9.3-6) vanishes. A more precise expression for σ_τ that incorporates the spread of the spectral width σ_λ about $\lambda_o = 1.312\ \mu$m yields a very small, but nonzero, width.

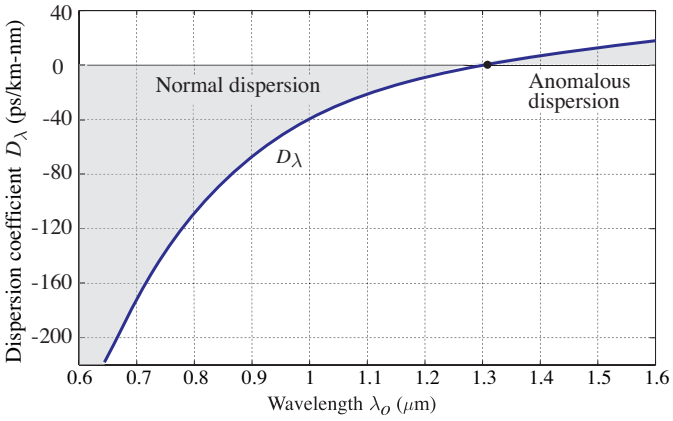

Figure 9.3-5 Dispersion coefficient D_λ for a silica-glass fiber as a function of wavelength λ_o. The result is similar to, but distinct from, that of fused silica (see Fig. 5.6-5).

EXAMPLE 9.3-2. ***Pulse Broadening Associated with Material Dispersion.*** The dispersion coefficient D_λ for a silica-glass fiber is approximately -80 ps/km-nm at $\lambda_o = 0.87\ \mu$m. For a source of spectral linewidth $\sigma_\lambda = 50$ nm (generated by an LED, for example) the pulse-spread rate in a single-mode fiber with no other sources of dispersion is $|D_\lambda|\sigma_\lambda = 4$ ns/km. An

impulse of light traveling a distance $L = 100$ km in the fiber is therefore broadened to a width $\sigma_\tau = |D_\lambda|\sigma_\lambda L = 0.4$ μs. The response time of the fiber is thus $\sigma_\tau = 0.4$ μs. As another example, an impulse with narrower spectral linewidth $\sigma_\lambda = 2$ nm (generated by a laser diode, for example), operating near 1.3 μm where the dispersion coefficient is 1 ps/km-nm, spreads at a rate of only 2 ps/km. In this case, therefore, a 100-km fiber has a substantially shorter response time, $\sigma_\tau = 0.2$ ns.

Combined Material and Modal Dispersion

The effect of material dispersion on pulse broadening in multimode fibers may be determined by returning to the original equations for the propagation constants β_q of the modes and determining the group velocities $v_q = (d\beta_q/d\omega)^{-1}$ with n_1 and n_2 given as functions of ω. Consider, for example, the propagation constants of a graded-index fiber with a large number of modes, which are given by (9.2-41) and (9.2-37). Although n_1 and n_2 are dependent on ω, it is reasonable to assume that the ratio $\Delta = (n_1 - n_2)/n_1$ is approximately independent of ω. Using this approximation and evaluating $v_q = (d\beta_q/d\omega)^{-1}$, we obtain

$$v_q \approx \frac{c_o}{N_1}\left[1 - \frac{p-2}{p+2}\left(\frac{q}{M}\right)^{p/(p+2)}\Delta\right], \tag{9.3-8}$$

where $N_1 = (d/d\omega)(\omega n_1) = n_1 - \lambda_o(dn_1/d\lambda_o)$ is the group index of the core material. Under this approximation, the earlier expression (9.2-43) for v_q remains intact, except that the refractive index n_1 is replaced with the group index N_1. For a step-index fiber $(p \to \infty)$, the group velocities of the modes vary from c_o/N_1 to $(c_o/N_1)(1-\Delta)$, so that the response time is

$$\boxed{\sigma_\tau \approx \frac{L}{(c_o/N_1)} \cdot \frac{\Delta}{2}.} \tag{9.3-9}$$

Response Time (Multimode Step-Index, Material Dispersion)

This expression should be compared with (9.3-4), which is applicable in the absence of material dispersion.

EXERCISE 9.3-1

Optimal Grade Profile Parameter. Use (9.2-41) and (9.2-37) to derive the following expression for the group velocity v_q when both n_1 and Δ are wavelength dependent:

$$v_q \approx \frac{c_o}{N_1}\left[1 - \frac{p-2-p_s}{p+2}\left(\frac{q}{M}\right)^{p/(p+2)}\Delta\right], \qquad q = 1, 2, \ldots, M \tag{9.3-10}$$

with $p_s = 2(n_1/N_1)(\omega/\Delta)\, d\Delta/d\omega$. What is the optimal value of the grade profile parameter p for minimizing modal dispersion?

Waveguide Dispersion

The group velocities of the modes in a waveguide depend on the wavelength even if material dispersion is negligible. This dependence, known as **waveguide dispersion**,

results from the dependence of the field distribution in the fiber on the ratio of the core radius to the wavelength (a/λ_o). The relative portions of optical power in the core and cladding thus depend on λ_o. Since the phase velocities in the core and cladding differ, the group velocity of the mode is altered. Waveguide dispersion is particularly important in single-mode fibers where modal dispersion is not present, and at wavelengths for which material dispersion is small (near $\lambda_o = 1.3\ \mu\text{m}$ in silica glass), since it then dominates.

As discussed in Sec. 9.2A, the group velocity $v = (d\beta/d\omega)^{-1}$ and the propagation constant β are determined from the characteristic equation, which is governed by the fiber V parameter, $V = 2\pi(a/\lambda_o)\text{NA} = (a \cdot \text{NA}/c_o)\omega$. In the absence of material dispersion (i.e., when NA is independent of ω), V is directly proportional to ω, so that

$$\frac{1}{v} = \frac{d\beta}{d\omega} = \frac{d\beta}{dV}\frac{dV}{d\omega} = \frac{a \cdot \text{NA}}{c_o}\frac{d\beta}{dV}. \tag{9.3-11}$$

The pulse broadening associated with a source of spectral width σ_λ is related to the time delay L/v by $\sigma_\tau = |(d/d\lambda_o)(L/v)|\sigma_\lambda$. Thus,

$$\sigma_\tau = |D_w|\sigma_\lambda L, \tag{9.3-12}$$

where the waveguide dispersion coefficient D_w is given by

$$D_w = \frac{d}{d\lambda_o}\left(\frac{1}{v}\right) = -\frac{\omega}{\lambda_o}\frac{d}{d\omega}\left(\frac{1}{v}\right). \tag{9.3-13}$$

Substituting (9.3-11) into (9.3-13) leads to

$$D_w = -\left(\frac{1}{2\pi c_o}\right)V^2\frac{d^2\beta}{dV^2}. \tag{9.3-14}$$

Thus, the group velocity is inversely proportional to $d\beta/dV$ and the waveguide dispersion coefficient is proportional to $V^2 d^2\beta/dV^2$. The dependence of β on V is displayed in Fig. 9.2-8(a) for the fundamental LP_{01} mode. Since β varies nonlinearly with V, the waveguide dispersion coefficient D_w is itself a function of V and is therefore also a function of the wavelength.† The dependence of D_w on λ_o may be controlled by altering the radius of the core or, for graded-index fibers, the index grading profile.

Combined Material and Waveguide Dispersion

The combined effects of material dispersion and waveguide dispersion (which we refer to as **chromatic dispersion**) may be determined by including the wavelength dependence of the refractive indexes, n_1 and n_2 and therefore NA, when determining $d\beta/d\omega$ from the characteristic equation. Although generally smaller than material dispersion, waveguide dispersion does shift the wavelength at which the total chromatic dispersion is minimum.

Since chromatic dispersion limits the performance of single-mode fibers, more advanced fiber designs aim at reducing this effect by using graded-index cores with refractive-index profiles selected such that the wavelength at which waveguide dispersion compensates material dispersion is shifted to the wavelength at which the fiber is to be used. **Dispersion-shifted fibers** have been successfully fabricated by using a linearly tapered core refractive index and a reduced core radius, as illustrated in Fig. 9.3-6(a). This technique can be used to shift the zero-chromatic-dispersion

† For further details on this topic, see the reading list, particularly the articles by Gloge.

wavelength from $1.3\ \mu\text{m}$ to $1.55\ \mu\text{m}$, where the fiber has its lowest attenuation. Other grading profiles have been developed for which the chromatic dispersion vanishes at two wavelengths and is reduced for intermediate wavelengths. These fibers, called **dispersion-flattened**, have been implemented by using a quadruple-clad layered grading, as illustrated in Fig. 9.3-6(b). Note, however, that the process of index grading itself introduces losses since dopants are used.

Fibers with other refractive index profiles may be engineered such that the combined material and waveguide dispersion coefficient is proportional to that of a conventional step-index fiber but has the opposite sign. This can be achieved over an extended wavelength band, as illustrated in Fig. 9.3-6(c). The pulse spread introduced by a conventional fiber can then be reversed by concatenating the two types of fiber. A fiber with a reversed dispersion coefficient is known as a **dispersion compensating fiber** (**DCF**). A short segment of the DCF may be used to compensate the dispersion introduced by a long segment of conventional fiber.

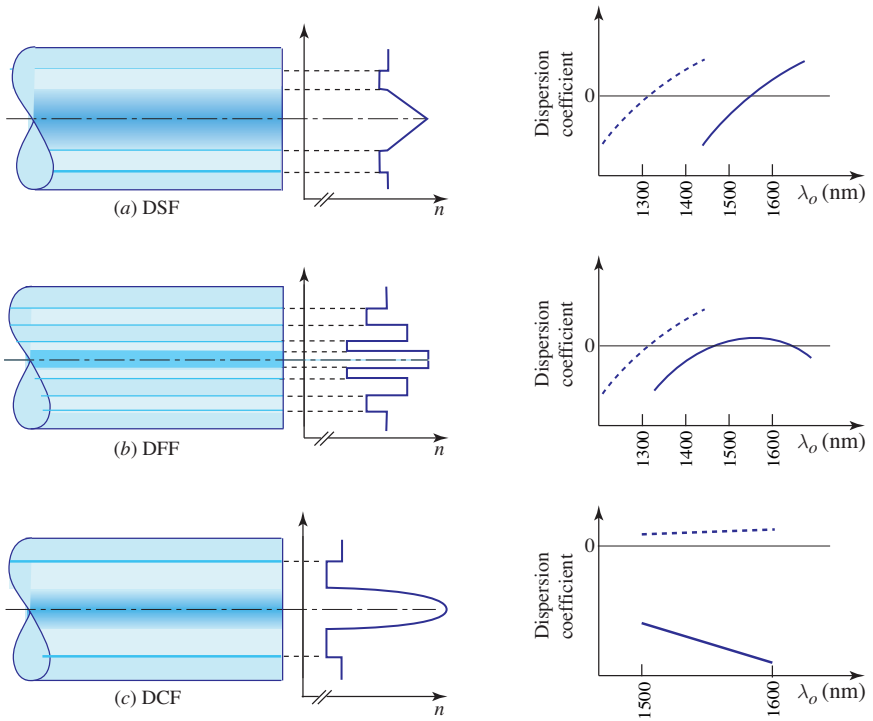

Figure 9.3-6 Refractive-index profiles with schematic wavelength dependences of the material dispersion coefficient (dashed curves) and the combined material and waveguide dispersion coefficients (solid curves) for (a) dispersion-shifted fiber (DSF), (b) dispersion-flattened fiber (DFF), and (c) dispersion-compensating fiber (DCF).

Polarization Mode Dispersion (PMD)

As indicated earlier, the fundamental spatial mode (LP_{01}) of an optical fiber has two polarization modes, say linearly polarized in the x and y directions. If the fiber has perfect circular symmetry about its axis, and its material is perfectly isotropic, then the two polarization modes are degenerate, i.e., they travel with the same velocity. However, fibers exposed to real environmental conditions exhibit a small birefringence that

varies randomly along their length. This is caused by slight variations in the refractive indexes and fiber cross-section ellipticity. Although the effects of such inhomogeneities and anisotropies on the polarization modes, and on the dispersion of optical pulses, are generally difficult to assess, we consider these effects in terms of simple models.

Consider first a fiber modeled as a homogeneous anisotropic medium with principal axes in the x and y directions and principal refractive indexes n_x and n_y. The third principal axis lies, of course, along the fiber axis (the z direction). The fiber material is assumed to be dispersive so that n_x and n_y are frequency dependent, but the principal axes are taken to be frequency independent within the spectral band of interest. If the input pulse is linearly polarized in the x direction, over a length of fiber L, it will undergo a group delay $\tau_x = N_x L/c_o$; if it is linearly polarized in the y direction, the group delay will be $\tau_y = N_y L/c_o$. Here, N_x and N_y are the group indexes associated with n_x and n_y (see Sec. 5.6). A pulse in a polarization state that includes both linear polarizations will undergo a **differential group delay** (**DGD**) $\delta\tau = |\tau_y - \tau_x|$ given by

$$\boxed{\delta\tau = \Delta N L/c_o,} \qquad (9.3\text{-}15)$$

Differential Group Delay

where $\Delta N = |N_y - N_x|$. Upon propagation, therefore, the pulse will split into two orthogonally polarized components whose centers will separate in time as the pulses travel (see Fig. 9.3-7). The DGD corresponds to **polarization mode dispersion** (PMD) that increases linearly with the fiber length at the rate $\Delta N/c_o$, which is usually expressed in units of ps/km.

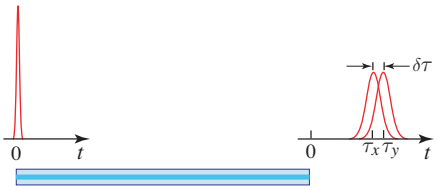

Figure 9.3-7 Differential group delay (DGD) associated with polarization mode dispersion (PMD).

Since a long fiber is typically exposed to environmental and structural factors that vary along its axis, the simple model considered above is often inadequate. Under these conditions, a more realistic model comprises a sequence of short homogeneous fiber segments, each with its own principal axes and principal indexes. The principal axes are taken to be slightly misaligned (rotated) from one segment to the next. Such a cascaded system is generally described by a 2×2 Jones matrix $\mathbf{T}$, which is a product of the Jones matrices of the individual segments (see Sec. 6.1B). The polarization modes of the combined system are the eigenvectors of $\mathbf{T}$ and are not necessarily linearly polarized modes. If the fiber is taken to be lossless, the matrix $\mathbf{T}$ is unitary. Its eigenvalues are then phase factors $\exp(j\varphi_1)$ and $\exp(j\varphi_2)$, which may be written in the form $\exp(jn_1k_oL)$ and $\exp(jn_2k_oL)$, where n_1 and n_2 are the effective refractive indexes of the two polarization modes and L is the fiber length. The propagation of light through such a length of fiber may then be determined by analyzing the input wave into components along the two polarization modes; these components travel with effective refractive indexes n_1 and n_2.

Since the fiber is dispersive, $\mathbf{T}$ is frequency dependent and so too are the indexes n_1 and n_2 of the modes, as well as their corresponding group indexes N_1 and N_2. An input pulse with a polarization state that is the same as that of the fiber's first polarization mode travels with an effective group index N_1. Similarly, if the pulse is in the second polarization mode, it travels with an effective group index N_2. However, an input pulse

with a component in each of the fiber's polarization modes suffers DGD, as provided in (9.3-15), with $\Delta N = |N_1 - N_2|$.

A statistical model describing the random variations in the magnitude and orientation of birefringence along the length of the fiber leads to an expression of the RMS value of the pulse broadening associated with DGD. This turns out to be proportional to $\sqrt{L}$ instead of L,

$$\sigma_{\text{PMD}} = D_{\text{PMD}}\sqrt{L}, \tag{9.3-16}$$

Polarization-Mode Dispersion

where D_{PMD} is a dispersion parameter typically ranging from 0.1 to 1 ps/$\sqrt{km}$.

Aside from DGD, higher-order dispersion effects are also present. Each of the polarization modes is spread by group-velocity dispersion (GVD) with dispersion coefficients proportional to the second derivative of its refractive index (see Sec. 5.6).

Another higher-order effect relates to the coupled nature of the spectral and polarization properties of the system. Since the matrix $\mathbf{T}$ is frequency dependent, not only are the eigenvalues (i.e., the principal indexes n_1 and n_2) frequency dependent, but so too are the eigenvectors (i.e., the polarization modes). If the pulse spectral width is sufficiently narrow (i.e., the pulse is not too short), we may approximately use the polarization modes at the central frequency. For ultrashort pulses, however, a more detailed analysis that includes a combined polarization and spectral description of the system is required. Polarization states may be found such that the group delays are frequency insensitive so that their associated GVD is minimal. However, these are not eigenvectors of the Jones matrix so that the input and output polarization states are not the same.†

EXERCISE 9.3-2

Differential Group Delay in a Two-Segment Fiber. Consider the propagation of an optical pulse through a fiber of length 1 km comprising two segments of equal length. Each segment is a single-mode anisotropic fiber with principal group indexes $N_x = 1.462$ and $N_y = 1.463$. The corresponding group velocity dispersion coefficients are $D_x = D_y = 20$ ps/km-nm. The principal axes of one segment are at an angle of 45° with respect to the other, as illustrated in Fig. 9.3-8.

(a) If the input pulse has a width of 100 ps and is linearly polarized at 45° with respect to the fiber x and y directions, sketch the temporal profile of the pulse at the output end of the fiber. Assume that the pulse source has a spectral linewidth of 50 nm.

(b) Determine the polarization modes of the full fiber and determine the temporal profile of the output pulse if the input pulse is in one of the polarization modes.

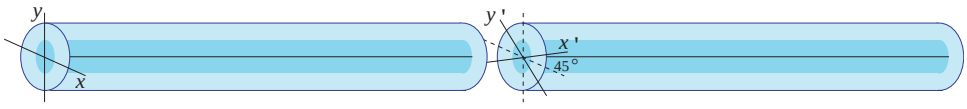

Figure 9.3-8 Two-segment birefringent fiber.

† For more details on this topic, see C. D. Poole and R. E. Wagner, Phenomenological Approach to Polarization Dispersion in Long Single-Mode Fibers, *Electronics Letters*, vol. 22, pp. 1029-1030, 1986.

Nonlinear Dispersion

Yet another dispersion effect occurs when the intensity of light in the core of the fiber is sufficiently high, since the refractive index then becomes intensity dependent and the material exhibits nonlinear behavior. Since the phase is proportional to the refractive index, the high-intensity portions of an optical pulse undergo phase shifts different from the low-intensity portions, resulting in instantaneous frequencies shifted by different amounts. This nonlinear effect, called **self-phase modulation** (SPM), contributes to pulse dispersion. Under certain conditions, SPM can compensate the group velocity dispersion (GVD) associated with material dispersion, and the pulse can travel without altering its temporal profile. Such a guided wave is known as a soliton. Nonlinear optics is introduced in Chapter 21 and optical solitons are discussed in Chapter 22.

Summary

The propagation of pulses in optical fibers is governed by attenuation and several types of dispersion. Figure 9.3-9 provides a schematic illustration in which the profiles of pulses traveling through different types of fibers are compared.

- In a multimode fiber (MMF), modal dispersion dominates and the width of the pulse received at the terminus of the fiber. It is governed by the disparity in the group delays of the individual modes.
- In a single-mode fiber (SMF), there is no modal dispersion and the transmission of optical pulses is limited by combined material and waveguide dispersion (called chromatic dispersion). The width of the output pulse is governed by group velocity dispersion (GVD).
- Material dispersion is usually much stronger than waveguide dispersion. However, at wavelengths where material dispersion is small, waveguide dispersion becomes important. Fibers with special index profiles may then be used to alter the chromatic dispersion characteristics, creating dispersion-flattened, dispersion-shifted, and dispersion-compensating fibers.
- Pulse propagation in long single-mode fibers for which chromatic dispersion is negligible is dominated by polarization mode dispersion (PMD). Small anisotropic changes in the fiber, caused, for example, by environmental conditions, alter the polarization modes so that the input pulse travels in two polarization modes with different group indexes. This differential group delay (DGD) results in a small pulse spread.
- Under certain conditions an intense pulse, called an optical soliton, can render a fiber nonlinear and travel through it without broadening. This results from a balance between material dispersion and self-phase modulation (the dependence of the refractive index on the light intensity), as discussed in Chapter 22.

9.4 HOLEY AND PHOTONIC-CRYSTAL FIBERS

A **holey fiber** is a pure silica-glass fiber that contains multiple cylindrical air holes parallel to, and along the length of, its axis. The holes are organized in a regular periodic pattern. As illustrated in Fig. 9.4-1, the core is defined by a **defect**, or fault,

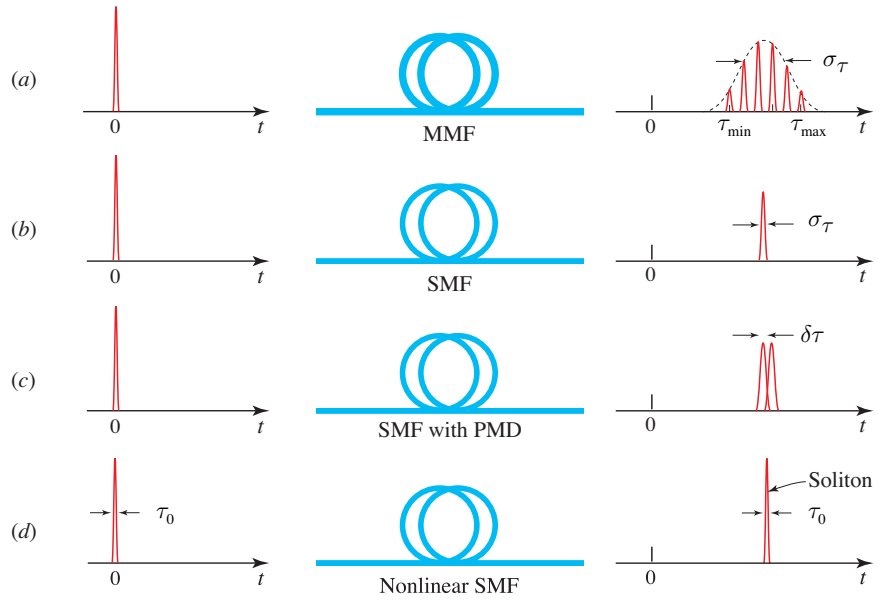

Figure 9.3-9 Broadening of a short optical pulse after transmission through different types of fibers. (*a*) Modal dispersion in a multimode fiber (MMF). (*b*) Material and waveguide dispersion in a single-mode fiber (SMF). (*c*) Polarization mode dispersion (PMD) in a SMF. (*d*) Soliton transmission in a nonlinear SMF.

in the periodic structure, such as a missing hole, a hole of a different size, or an extra hole. The holes are characterized by the spacing between their centers, Λ, and their diameters, d. The quantity Λ, which is also called the **pitch**, is typically in the range 1–10 μm. It is not necessary to include dopants in the glass.

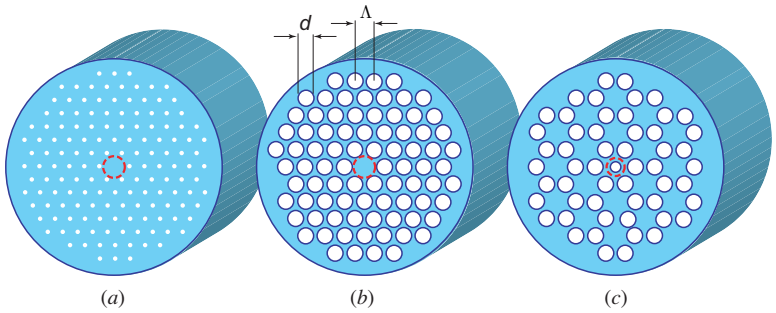

Figure 9.4-1 Various forms of holey fibers. (*a*) Solid core (dotted circle) surrounded by a cladding of the same material but suffused with a periodic array of cylindrical air holes whose diameters are much smaller than a wavelength. The average refractive index of the cladding is lower than that of the core. (*b*) Photonic-crystal holey fiber with cladding that contains a periodic array of large air holes and a solid core (dotted circle). (*c*) Photonic-crystal holey fiber with cladding that contains a periodic array of large air holes and a core that is an air hole of a different size (dotted circle).

Holey fibers guide optical waves via one of two mechanisms: **effective-index guidance** and **photonic-bandgap guidance**, which we consider in turn below.

Effective-Index Guidance

If the hole diameter is much smaller than the wavelength of light ($d \ll \lambda$), then the periodic cladding behaves approximately as a homogeneous medium whose **effective refractive index** n_2 is equal to the average refractive index of the holey material [see Fig. 9.4-1(a)]. Waveguiding is then achieved by making use of a solid core with index $n_1 > n_2$, so that the light is guided by total internal reflection as with conventional fibers. In this configuration, the holes serve merely as distributed "negative dopants" that reduce the refractive index of the cladding below that of the solid core. The holes can therefore be randomly, rather than periodically, arrayed and they need not be axially continuous.

If the size of the holes is not much smaller than the wavelength, then the holey cladding must be treated as a two-dimensional periodic medium. The effective refractive index n_2 is then equal to the average refractive index, weighted by the optical intensity distribution in the medium, and is therefore strongly dependent on the wavelength as well as on the size and the geometry of the holes. Since waves of shorter wavelength are more confined in the medium of higher refractive index, the effective refractive index of the cladding $n_2(\lambda)$ is a decreasing function of the wavelength. A similar effect occurs in a 1D photonic crystal, for which the effective refractive index is an increasing function of frequency at frequencies in the lowest photonic band (see Fig. 7.2-6). The holey fiber is therefore endowed with strong waveguide dispersion, which can be an extremely useful feature.

One consequence of the waveguide dispersion is that the holey fiber may operate as a single-mode structure over a broad range of wavelengths, possibly stretching from the infrared to the ultraviolet.[†] This property, called **endless single-mode guidance**, results when the fiber V parameter, $V = (2\pi a/\lambda)\sqrt{n_1^2 - n_2^2(\lambda)}$, is approximately independent of λ. This condition arises when the effective index $n_2(\lambda)$ decreases with λ in such a way that $\sqrt{n_1^2 - n_2^2(\lambda)} \propto \lambda$. For a conventional fiber, in contrast, V is inversely proportional to λ so that single-mode behavior at a particular wavelength ($V < 2.405$) morphs into multimode behavior for a sufficiently lower wavelength such that V increases above 2.405.

Another interesting feature is the feasibility of **large mode-area** (LMA) single-mode operation. Optical fibers with large mode areas are useful for applications requiring high power delivery. In a conventional fiber the condition of single-mode operation ($V = 2\pi(a/\lambda_o)\mathrm{NA} < 2.405$) can be met for a large core diameter $2a$ by use of a small numerical aperture. Similarly, the guided mode size can be increased in holey fibers by having a larger hole-to-hole spacing Λ (thus resulting in a larger core diameter) and using holes with smaller diameter d (creating a lower numerical aperture and allowing the field to penetrate farther into the cladding). Dramatic increases in mode area for relatively small changes in the hole size are obtained and mode areas that are several order of magnitudes greater than in conventional fibers have been reported.

Photonic-Bandgap Guidance

The cladding of a holey fiber may be regarded as a two-dimensional **photonic crystal**. The triangular-hole microstructure shown in Fig. 9.4-1(b), for example, has a dispersion diagram with photonic bandgaps, as shown in Fig. 7.3-3 and discussed in Sec. 7.3A. If the optical frequency lies within the photonic bandgap, propagation through the cladding is prohibited and the fiber serves as a photonic-crystal waveguide (see Sec. 8.5).

A **photonic-crystal fiber** (PCF) may have a solid or hollow core, as illustrated in Fig. 9.4-1(b) and (c), respectively. Fibers with a hollow core are novel since they cannot

[†] See T. A. Birks, J. C. Knight, and P. St. J. Russell, Endlessly Single-Mode Photonic Crystal Fibre, *Optics Letters*, vol. 22, pp. 961–963, 1997.

operate by effective-index guidance; i.e., guidance cannot be based on total internal reflection. A guided wave traveling in an air-core PCF suffers lower losses and reduced nonlinear effects, and can carry increased amounts of optical power. As a result, PCFs offer many unique design possibilities. Dispersion flattening over broad wavelength ranges can be achieved as can dispersion shifting to wavelengths lower than the zero-material-dispersion wavelength. Powerful fiber lasers that operate over a broad range of wavelengths can be constructed. A whole raft of other applications are also possible, such as analyzing gases by introducing them into the fiber core.

READING LIST

Books

See also the books on optical waveguides in Chapter 8.

C. DeCusatis and C. J. Sher DeCusatis, *Fiber Optic Essentials*, Elsevier, 2005.

J. Hecht, *Understanding Fiber Optics*, Prentice Hall, 5th ed. 2005.

F. Zolla, G. Renversez, A. Nicolet, B. Kuhlmey, S. Guenneau, and D. Felbacq, *Foundations of Photonic Crystal Fibres*, Imperial College Press (London), 2005.

A. Galtarossa and C. R. Menyuk, eds., *Polarization Mode Dispersion*, Springer-Verlag, 2005.

R. P. Khare, *Fiber Optics and Optoelectronics*, Oxford University Press, 2004.

J. A. Buck, *Fundamentals of Optical Fibers*, Wiley, 1995, 2nd ed. 2004.

J. Hecht, *City of Light: The Story of Fiber Optics*, Oxford University Press, 2004.

A. Bjarklev, J. Broeng, and A. S. Bjarklev, *Photonic Crystal Fibers*, Springer-Verlag, 2003.

J. K. Petersen, *Fiber Optics Illustrated Dictionary*, CRC Press, 2003.

I. Kaminow and T. Li, eds. *Optical Fiber Telecommunications IVA: Components*, Academic Press, 2002.

C. Manolatou and H. A. Haus, *Passive Components for Dense Optical Integration*, Kluwer, 2002.

D. R. Goff and K. S. Hansen. eds., *Fiber Optic Reference Guide: A Practical Guide to the Technology*, Focal, 3rd ed. 2002.

R. Tricker, *Optoelectronics and Fiber Optic Technology*, Newnes, 2002.

R. J. Bates, *Basic Fiberoptics Technologies*, McGraw–Hill, 2001.

J. Crisp, *Introduction to Fiber Optics*, Newnes, 2nd ed. 2001.

A. Othonos and K. Kalli, *Fiber Bragg Gratings: Fundamentals and Applications in Telecommunications and Sensing*, Artech, 1999.

A. Ghatak and K. Thyagarajan, *An Introduction to Fiber Optics*, Cambridge University Press, 1998.

J. S. Sanghera and I. D. Aggarwal, eds., *Infrared Fiber Optics*, CRC Press,1998.

J. P. Powers, *An Introduction to Fiber Optic Systems*, Irwin, 2nd ed. 1997.

M. H. Weik, *Fiber Optics Standard Dictionary*, Chapman & Hall, 3rd ed. 1997.

A. Kumar, *Antenna Design with Fiber Optics*, Artech House, 1996.

J. L. Miller and E. Friedman, *Photonics Rules of Thumb: Optics, Electro-Optics, Fiber Optics, and Lasers*, McGraw–Hill, 1996.

C.-L. Chen, *Elements of Optoelectronics and Fiber Optics*, Irwin, 1995.

R. B. Dyott, *Elliptical Fiber Waveguides*, Artech House, 1995.

N. Kashima, *Passive Optical Components for Optical Fiber Transmission*, Artech, 1995.

S. G. Krivoshlykov, *Quantum-Theoretical Formalism for Inhomogeneous Graded-Index Waveguides*, Akademie-Verlag, 1994.

G. Cancellieri, *Single-Mode Optical Fiber Measurement: Characterization and Sensing*, Artech House, 1993.

J. E. Midwinter, *Optical Fibers for Transmission*, Wiley, 1979; Krieger, reissued 1992.

K. Chang, ed., *Fiber and Electro-Optical Components*, Wiley, 1991.

P. K. Cheo, *Fiber Optics and Optoelectronics*, Prentice Hall, 1985, 2nd ed. 1990.